



27 **1 Introduction**

28 Carbonyl compounds are a group of oxygenated volatile organic compounds (OVOCs) that are emitted into the
29 atmosphere from natural and anthropogenic sources (Bao et al., 2022), but they are also formed in the atmosphere
30 as oxidation products of other volatile organic compounds (VOCs) (Mellouki et al., 2015). It is well established that
31 OVOCs play an important role in the sequence of chemical reactions that leads to their further oxidation and
32 contributes to the tropospheric ozone formation in polluted and remote environments with important effect on health
33 as is the case of formaldehyde and acetaldehyde (Calvert et al., 2011, Liu et al., 2022, Mellouki et al., 2015, Zhou
34 et al., 2023). In addition, large carbonyl compounds can influence on climate change if they are strong infrared light
35 absorbers by altering the Earth's radiation balance and being an important source of aerosol which could further
36 affect radiation balance and be hazardous for health (Heald and Kroll, 2020, Liu et al., 2022;).

37 The rising O₃ levels in mega-city clusters like Chinese cities underscore the critical need for effective control of
38 ambient carbonyls, significant precursors of O₃. Moreover, as intermediate products of hydrocarbon oxidation,
39 carbonyls likely play a pivotal role in minimizing the disparity between atmospheric reactivity in measurements and
40 simulations. Previous studies (Calvert et al., 2011, Liu et al., 2022, Mellouki et al., 2015, Zhou et al., 2023) have
41 provided valuable insights into carbonyls' presence, composition, origins, and impact on O₃ and SOA formation,
42 using a combination of field measurements, numerical simulations, and laboratory experiments. Nevertheless,
43 further research is still warranted to achieve a more comprehensive understanding of carbonyls' sources and sinks,
44 given the complexity of their emission and degradation processes (Liu et al., 2022).

45 In this work, the tropospheric reactivity of two carbonyls compounds whose reactivity is not yet completely
46 established, has been studied: 3,3-dimethylbutanal (33DMButanal) and 3,3-dimethylbutanone (33DMButanone).
47 These two carbonyls are among the reaction products identified in the atmospheric degradation of two alcohols (3,3-
48 dimethyl-1-butanol and 3,3-dimethyl 2-butanol), which reactivity have been previously studied (by our research
49 group) (Colmenar et al 2020). On the other hand, 3,3-dimethylbutanal has also been detected as reaction product in
50 the reaction of 2,4,4-trimethyl-1-pentanol with Cl atoms (Vila et al., 2020) and it could be an intermediate in the
51 synthesis of neotame, a sweetener (Tanielyan and Augustine, 2012). Industrially, 33DMbutanone, known as methyl
52 tert-butyl ketone, is produced for use in fungicides, herbicides and pesticides (Liu et al., 2022) and it might also be
53 a solvent for the extraction of methylphenols from wastewater (Xiong et al. 2018). Specifically, in the study of Byrne
54 et al. (2018) 33DMbutanone has been identified as potential replacements for hazardous volatile non-polar solvents
55 such as toluene, due to low toxicity and good solvation characteristics. In addition to direct emissions,
56 33DMbutanone could be present in the atmosphere as a reaction product of the gas-phase oxidation of 2,2-
57 dimethylbutane (Jenkin et al., 1997, Saunders et al., 2003) and 3,3-dimethyl-2-butanol (Colmenar et al. 2020).

58 Specifically, for 33DMButanal and 33DMbutanone few studies about their atmospheric reactivity have been
59 reported in the literature. In the case of the reaction of 33DMbutanal with OH radical, the experimental rate
60 coefficient has been measured by Aschmann et al. (2010) and D'Anna et al., (2001). Only one study on the reaction
61 products with OH radicals has been reported by Aschmann et al., (2010). For the reaction of 33DMButanal with
62 NO₃ radical two kinetic studies are available in the literature (D'Anna et al., 2001, D'Anna and Nielsen 1997). Tadic
63 et al., 2012 has reported the photochemical parameters of 33DMbutanal due to the importance of the
64 photodissociation of aldehydes in the atmosphere since it could represent an important source of free radicals. To
65 our knowledge, there are no data about the reaction of 33DMbutanal with Cl atoms.



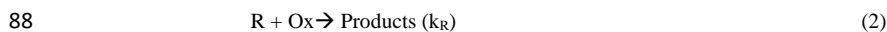
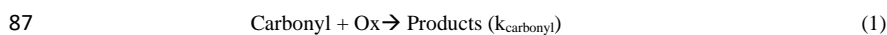
66 In the case of 33DMButanone only a kinetic study with Cl atoms has been carried out (Farrugia et al., 2015) and
67 two studies with OH radicals (Mapelli et al., 2023; Wallington and Kurylo 1987). In the OH studies, the rate
68 coefficient has been obtained at different temperatures and at low pressure, using absolute methods. No studies have
69 been carried out on the products of Cl atom and OH radical reaction with 33DMButanone that could help to establish
70 the reaction mechanisms.

71 Taking the above into consideration, the aim of this work is to complete the studies about the reactivity of
72 33DMButanal and 33DMButanone to further understand their atmospheric chemistry in particular and the carbonyls
73 in general. For this purpose, the kinetic study has been conducted for the reactions of 33DMButanal and
74 33DMButanone with Cl atoms and 33DMButanone with OH radicals using a relative method and FTIR technique
75 as detection system. Additionally, for the reactions of 33DMButanal with Cl atoms, OH and NO₃ radicals and for
76 the reactions of 33DMButanone with Cl atoms and OH radicals a complete reaction product study has been
77 performed using FTIR and GC-TOFMS techniques. This work is to date the first kinetic study reported in
78 bibliography for the reaction of 33DMButanal with Cl atoms and the first study on reaction products and mechanisms
79 for the reactions of 33DMButanone with Cl atoms and OH radicals, and 33DMButanal with Cl atoms and NO₃
80 radicals. Additionally, this work includes a study on the reaction products for the reaction of 33DMButanal with OH
81 radicals in order to confirm the mechanism proposed by Aschmann et al., (2010).

82 2 Experimental Section

83 2.1 Rate coefficients determination: relative method

84 Rate coefficients have been determined using a relative rate method on the assumption that the organic compound
85 (carbonyl: 33DMButanal or 33DMbutanone), and the reference compound (R) are removed solely by their reactions
86 with the oxidants (Ox: Cl or ·OH):



89 where k_{carbonyl} and k_{R} are the rate coefficients of the carbonyl and the reference compound, respectively. The kinetic
90 treatment for the reactions (1) and (2) gives the following relationship:

$$91 \quad \ln \left(\frac{[\text{carbonyl}]_0}{[\text{carbonyl}]_t} \right) = \frac{k_{\text{carbonyl}}}{k_{\text{R}}} \times \ln \left(\frac{[\text{R}]_0}{[\text{R}]_t} \right) \quad (I)$$

92 where $[\text{carbonyl}]_0$, $[\text{R}]_0$, $[\text{carbonyl}]_t$, $[\text{R}]_t$, are the initial concentrations and those at time t for the carbonyl and the
93 reference compound, respectively. At least three reference compounds were employed for each studied reaction, and
94 the experiments were performed in triplicate for each one. According to eq. (I), a plot of $\ln([\text{carbonyl}]_0/[\text{carbonyl}]_t)$
95 versus $\ln([\text{R}]_0/[\text{R}]_t)$ (or a proportional property) should give a linear fit with an intercept equal to zero. The slope of
96 the plot corresponds to the ratio of the rate coefficients ($k_{\text{carbonyl}}/k_{\text{R}}$). Therefore, the value of k_{carbonyl} can be determined
97 if the rate coefficient of the reference compound (k_{R}) is known.

98 2.2 Experimental systems and procedure

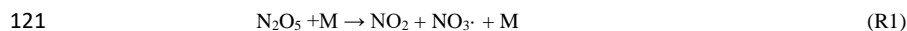


99 Kinetic and product studies were performed at room temperature (298 ± 5 K) and atmospheric pressure (710 ± 18
100 Torr) employing a 50 L Pyrex® glass cell as reaction chamber coupled to a FTIR spectrometer (Thermo, Nicolet
101 6700). Additionally, for products identification, samples of the reactions were taken using a Solid Phase
102 MicroExtraction fiber (SPME) as preconcentration sampling method and carried to a Gas Chromatograph coupled to
103 a Mass Spectrometer with Time Of Flight analyzer (GC-MSTOF) (AccuTOF GCv Jeol). Experimental details can
104 be found in previous publications (Aranda et al., 2020, Aranda et al., 2024, Colmenar et al., 2018, 2020a, 2020b).
105 Therefore, only a brief description is provided.

106 For FTIR experiments, the Pyrex® gas cell used contains a multireflection system that allows a maximum optical
107 path of 200 m (Saturn Series Multi-Pass cell). For the FTIR spectra collection, a total of 60 interferograms were co-
108 added over 98 s, usually taken in the range of $650\text{--}4000$ cm^{-1} with a resolution of 1 cm^{-1} . The passive sampling was
109 carried out using a Grey SPME fiber (DVB/CAR/PDMS). After the adsorption process (5-8 minutes of adsorption),
110 the fiber was taken to the injection port of the gas chromatograph (GC), where the compounds were desorbed at 250
111 $^{\circ}\text{C}$, separated and detected by GC-MSTOF. Two different capillary columns with the same characteristics were used:
112 a TRB-1701 (Teknokroma, $30\text{ m} \times 0.32\text{ mm} \times 1\text{ }\mu\text{m}$) and a Equity™ – 1701 (Supelco, $30\text{ m} \times 0.32\text{ mm} \times 1\text{ }\mu\text{m}$).
113 Once in the mass spectrometer, the compounds were ionized (Electron Ionization (EI) and/or Field Ionization (FI))
114 and fragmented to obtain their mass spectrum. The chromatographic conditions used for the analysis were as follows:
115 injection port, 250 $^{\circ}\text{C}$; interface, 250 $^{\circ}\text{C}$; oven initial temperature of 40 $^{\circ}\text{C}$ for 4 min; ramp, 25 $^{\circ}\text{C min}^{-1}$ to 120 $^{\circ}\text{C}$,
116 held for 10 min; second ramp, 20 $^{\circ}\text{C min}^{-1}$ to 200 $^{\circ}\text{C}$, held for 2 min.

117 The oxidants were generated by photolysis ($\lambda=350$ nm) of molecular chlorine (Cl_2) for reactions with Cl atoms and
118 by methyl nitrite (CH_3ONO) in the presence of O_2 and NO, for reactions with OH radicals. Some experiments have
119 been carried out using H_2O_2 as precursor of OH and UV radiation ($\lambda=254$ nm) in a Quartz gas cell reactor.

120 The decomposition of dinitrogen pentoxide was used as source of NO_3 radical according to reaction 1.



122 The kinetic experiments were conducted in a nitrogen atmosphere for reactions with Cl atoms, while synthetic air
123 was used for reactions with OH radicals. All the experiments conducted for the study of products were carried out
124 in synthetic air.

125 The reactions were followed by measuring the absorbance of the characteristic IR bands of each organic compound
126 (33DMbutanal/33DMbutanone and the reference compounds in the case of kinetic analysis) at different reaction
127 times. The IR spectra were processed using OMNIC software, through a subtraction procedure of the IR bands.

128 The concentration ranges (in ppm) used in the kinetic experiments were: 10-12 for 33DMbutanal and
129 33DMbutanone, 9-10 for 1-butene, 10-14 for Propene, 35-40 for 2-methylpropene, 13-14 for Isopropanol, 10-17 for
130 Cyclohexane, 5-14 for Propanal, 9-9.5 for 2-methyl-2-butanol, 5-6 for Ethyl formate, 11-15 for 1-butanol, 17-22 for
131 Cl_2 , 15-20 for NO and 16-20 for methyl nitrite. In the case of the reaction product experiments, the typical
132 concentration (in ppm) were: 10-14 for 33DMbutanal and 33DMbutanone; 22 for Cl_2 , 15-20 for NO, 16-20 for
133 methyl nitrite, 30 for H_2O_2 and for 14-25 for N_2O_5 .

134 2.3 Materials



135 Information on the purity and supplier company of the reagents used to carry out the experiments is specified below:
136 33DMbutanal (95%), 33DMbutanone (97%), and the reference compounds: 1-butene and Propene ($\geq 99\%$); 2-
137 methylpropene ($\geq 99.5\%$); Isopropanol (70% in H₂O), Propanal (97%), Cyclohexane (99.5%), 2-methyl-2-butanol
138 ($\geq 99\%$), Ethyl formate (97 %) and 1-butanol ($\geq 99\%$), 2,2-dimethylpropanoic acid (99%), 3,3-dimethylbutanoic acid
139 (98%) from Sigma Aldrich, Acetone ($\geq 99.5\%$) from Supelco. 22DMpropanal ($>95\%$) from TCI. The precursors of
140 the radicals were: methyl nitrite, CH₃ONO, synthesized in the laboratory according to the method of Taylor et al.,
141 (1980); and Cl₂ (99%) from Praxair. NO (98.5%) from Air Liquide, H₂O₂ (50 wt. % in H₂O, stabilized) from Sigma
142 Aldrich; N₂ (99.999%) and synthetic air (99.999%) from Praxair. Dinitrogen pentoxide (N₂O₅) synthesized in the
143 laboratory according to the procedure described by Schott and Davids (1958).

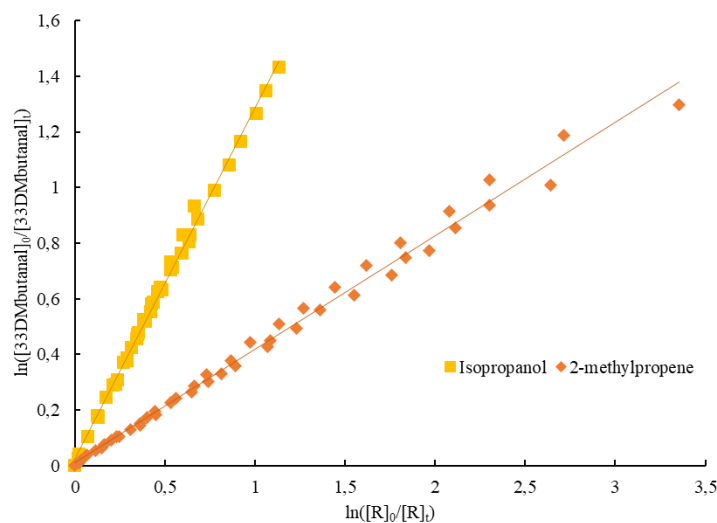
144 **3 Results and discussion**

145 **3.1 Kinetic study**

146 The reference compounds have been selected according to the following conditions: first that at least one active IR
147 band does not overlap with those of the compound under study (33DMbutanal or 33DMbutanone) and second, that
148 $0.1 \leq k_{\text{carbonyl}}/k_{\text{R}} \leq 10$. In addition, a series of experiments was carried out in order to evaluate possible heterogeneous
149 reactions with the walls, reactions between the compound under study and the reference compound, photolysis of
150 any of them and/or reactions with the oxidant precursor. The results of these experiments showed that the losses or
151 the reactants due to these processes were negligible ($< 3\%$ dark loss in the case of 33DMbutanal and 0% for
152 33DMbutanone).

153 The IR absorption bands used to follow the evolution of the different compounds were: 33DMbutanal, 2700 cm⁻¹;
154 1-butene, 911 cm⁻¹; propene, 878-942 cm⁻¹; 2-methylpropene 912 cm⁻¹; Isopropanol 1070 and 1251 cm⁻¹;
155 cyclohexane, 2862 and 2933 cm⁻¹, 33DMbutanona 1137 cm⁻¹, propanal 2710 cm⁻¹, 2-methyl-2-butanol 883 cm⁻¹,
156 ethyl formate 1192 and 1194 cm⁻¹, 1-butanol 1060 cm⁻¹.

157 The plots of $\ln([\text{carbonyl}]_0/[\text{carbonyl}]_t)$ versus $\ln([\text{R}]_0/[\text{R}]_t)$ for each reaction were generated according to equation
158 (I). As an example, in Figure 1 is shown the plot of equation (I) for the reaction of 33DMbutanal with Cl atoms with
159 the two reference compounds used. At least three reference compounds were used for each reaction, to assure the
160 accuracy of value determined. The reference compounds used, and the values of their rate coefficients are included
161 in Table 1. These values correspond to those recommended by McGillen et al., (2020).



162

163 Figure 1. Plot of Eq (1) for the reaction of 33DMbutanal with Cl atoms and for two reference compounds.

164 The slopes of the plots correspond to the relationship $k_{\text{carbonyl}}/k_{\text{R}}$, knowing the value of k_{R} , the rate coefficients of
 165 carbonyls can be determined. It can be seen the good linear fit with an intercept close to zero, indicating the absence
 166 of secondary reactions. The plots for the reaction of 33DMbutanone with Cl atoms and OH radical are shown in
 167 Figures 1S. The results obtained are shown in Table 1.

168 Table 1. Summary of relative and absolute rate coefficients for the reaction of 33DMbutanal with Cl atoms and
 169 33DMbutanone with Cl atoms and OH radicals. k in units of $\text{cm}^3 \text{ molecule}^{-1} \text{ s}^{-1}$.

Reaction	Reference compound ^d	$k_{\text{carbonyl}}/k_{\text{R}} \pm 2\sigma$	$k_{\text{carbonyl}} \pm 2\sigma^{\text{a,b,c}}$	
33DMbutanal+Cl ^a	2-methylpropene	0.38 ± 0.01	1.26 ± 0.27	
	$k_{\text{Cl}} = 3.3 \pm 0.7$	0.40 ± 0.01	1.32 ± 0.28	
		0.44 ± 0.01	1.46 ± 0.31	
		Isopropanol	1.38 ± 0.02	1.20 ± 0.31
	$k_{\text{Cl}} = 0.87 \pm 0.23$	1.25 ± 0.02	1.09 ± 0.28	
		1.27 ± 0.02	1.11 ± 0.29	
		Cyclohexane	0.43 ± 0.01	1.42 ± 0.22
	$k_{\text{Cl}} = 3.3 \pm 0.5$	0.36 ± 0.01	1.19 ± 1.18	
0.42 ± 0.02		1.40 ± 0.22		
Weighted Average			1.27 ± 0.08	
33DMbutanone+Cl ^b	Propanal	0.41 ± 0.02	5.10 ± 1.06	
	$k_{\text{Cl}} = 12.5 \pm 2.5$	0.37 ± 0.01	4.62 ± 0.93	
		0.42 ± 0.01	5.22 ± 1.06	
		0.42 ± 0.01	5.31 ± 1.07	
	2-methyl-2-butanol	0.42 ± 0.01	3.03 ± 0.76	
		$k_{\text{Cl}} = 7.30 \pm 1.80$	0.43 ± 0.01	3.10 ± 0.78
			0.47 ± 0.01	3.40 ± 0.85
Isopropanol	0.51 ± 0.02	4.41 ± 1.16		



	$k_{Cl} = 8.7 \pm 2.3$	0.48 ± 0.02	4.21 ± 1.10
		0.49 ± 0.01	4.22 ± 1.10
	Ethyl formate	4.87 ± 0.36	4.97 ± 1.05
	$k_{Cl} = 1.0 \pm 0.2$	4.93 ± 0.18	5.03 ± 1.02
		4.51 ± 0.32	4.60 ± 0.98
Weighted Average			4.22 ± 0.27
	Isopropanol	0.27 ± 0.01	1.39 ± 0.15
	$k_{OH} = 5.2 \pm 0.5$	0.22 ± 0.01	1.17 ± 0.12
		0.23 ± 0.02	1.18 ± 0.12
	2-methyl-2-butanol	0.49 ± 0.03	1.67 ± 0.51
	$k_{OH} = 3.4 \pm 1.0$	0.40 ± 0.02	1.38 ± 0.42
		0.56 ± 0.03	1.92 ± 0.59
33DMbutanone+OH ^c	1-butanol	0.14 ± 0.01	1.36 ± 0.28
	$k_{OH} = 9.8 \pm 2.0$	0.16 ± 0.01	1.62 ± 0.34
		0.18 ± 0.01	0.96 ± 0.11
	Cyclohexane	0.18 ± 0.01	1.23 ± 0.13
	$k_{OH} = 6.7 \pm 0.7$	0.15 ± 0.01	1.00 ± 0.11
		0.25 ± 0.03	1.67 ± 0.26
		0.23 ± 0.02	1.52 ± 0.20
Weighted Average			1.25 ± 0.05

170 ^{a, b, c} k_{carbonyl} and k_R is given in 10^{-10} , 10^{-11} , 10^{-12} , respectively. The data of k_R are values recommended by McGillen
 171 et al., (2020). The total absolute error $\sigma(k_{\text{carbonyl}})$ is a combination of the statistical errors from the regression analysis
 172 (σ_{slope}) and the quoted error in the value of the rate coefficient of the reference compound (σ_R). The final values of
 173 the rate coefficients and the associated error were calculated as weighted average.

174

175 To the best of our knowledge, this is the first work where the rate coefficient for the reaction of 33DMbutanal with
 176 Cl atoms is determined. On the other hand, the values of the rate coefficients of the reaction of 33DMbutanone with
 177 Cl atoms and OH radicals have been previously determined with values of $(0.48 \pm 0.05) \times 10^{-10} \text{ cm}^3 \text{ molecule}^{-1} \text{ s}^{-1}$
 178 (Farrugia et al., 2015) for Cl reaction and $(1.21 \pm 0.05) \times 10^{-12} \text{ cm}^3 \text{ molecule}^{-1} \text{ s}^{-1}$ (Wallington and Kurylo, 1987)
 179 and $(1.2 \pm 0.2) \times 10^{-12} \text{ cm}^3 \text{ molecule}^{-1} \text{ s}^{-1}$ (Mapelli et al., 2023) for OH reaction. These data are in good agreement
 180 with the values obtained in this study, thereby contributing to the accurate determination of the rate coefficients.

181 In the case of 33DMbutanone reactions the rate coefficient of Cl reactions ($4.22 \times 10^{-11} \text{ cm}^3 \text{ molecule}^{-1} \text{ s}^{-1}$) is one
 182 order of magnitude higher than the corresponding to OH reactions ($1.25 \times 10^{-12} \text{ cm}^3 \text{ molecule}^{-1} \text{ s}^{-1}$). This is the general
 183 trend observed in the atmospheric chemistry for the oxidation reactions of organic compounds; $k_{Cl} > k_{OH} \gg k_{NO_3}$. This
 184 behaviour can be explained by the higher reactivity and lower selectivity of chlorine atoms compared to the OH
 185 radical, where the site of attack determines its reactivity (Colmenar et al., 2020).

186 In Table 2, the rate coefficients for the reaction of different aldehydes and ketones in the butyl series with the main
 187 atmospheric oxidants have been tabulated to analyse the influence of the ramifications on reactivity.

188

189 Table 2. Rate coefficients for aldehydes and ketones in the butyl series with key atmospheric oxidants. k in units of
 190 $\text{cm}^3 \text{ molecule}^{-1} \text{ s}^{-1}$.

Aldehydes



Compounds	k_{Cl}^a	k_{OH}^b	$k_{NO_3}^c$
Butanal	1.66 ± 0.4^d	23.7 ± 5^d	1.10 ± 0.4^d
2-methylbutanal	2.16 ± 0.32^e	33.3 ± 13^d	2.67 ± 0.8^d
3-methylbutanal	2.07 ± 0.14^f	25.9 ± 5^d	2.19 ± 0.7^d
3,3-dimethylbutanal	1.27 ± 0.09^g	21.4 ± 9^d	1.77 ± 0.4^d

Ketones			
Compounds	k_{Cl}^a	k_{OH}^b	$k_{NO_3}^c$
2-butanone	0.40 ± 0.16^d	1.05 ± 0.2^d	
3-methylbutanone	0.68 ± 0.07^d	3.00 ± 1.2^d	$< 0.05^h$
3,3-dimethylbutanone	0.48 ± 0.05^d	1.21 ± 0.5^d	
	0.42 ± 0.03^g	1.25 ± 0.1^g	
		1.2 ± 0.2^i	

191 ^{a, b, c} k in 10^{-10} , 10^{-12} , 10^{-14} , respectively. ^dValues recommended in McGillen 2020. ^eAsensio et al., 2022. ^fBo et al.,
192 2022. ^gThis work. ^hGlasius et al., 1997. ⁱMapelli et al., 2023

193 For butanals, the trend in rate coefficient values indicates that the presence of a methyl group influences to the
194 reactivity, resulting in an increase in the rate coefficient compared to the compound without a methyl group. This
195 could be attributed to the activation of the hydrogen atom at the α - position by a methyl group, as noted in the
196 literature (Mellouki et al., 2015). Furthermore, the reactivity is influenced by both the position and quantity of methyl
197 groups. Consequently, the activating influence exerted by the methyl group on the hydrogen bonded to the carbon
198 adjacent to the aldehyde (α - position) is less pronounced when the methyl group occupies position 3 as opposed to
199 position 2. Basically, the impact of the methyl group manifests as a short-range activating effect. Regarding the
200 impact of the number of methyl groups on reactivity, in the case of 33DMbutanal, the significant decrease in the
201 value of rate coefficient with respect to 3-methylbutanal could be explained by an increase in steric hindrance,
202 making the hydrogen abstraction process at the α - position less probable, thereby resulting in lower reactivity
203 compared to the compound with one methyl group (3-methylbutanal).

204 Concerning butanones, no data are available for reactions with NO_3 radicals, with only one value for the upper limit
205 of 3-methylbutan-2-one (Glasius et al., 1997). The fact that the reactions of ketones with NO_3 radicals are too slow
206 complicates their experimental study and therefore, the determination of their rate coefficients. The available data
207 of rate coefficients for reactions of butanones with Cl atoms and OH radicals, show again that the presence of a
208 methyl group attached to a carbon in the α - position with respect to the carbonyl group activates the abstraction of
209 one hydrogen atom from this carbon, resulting in an increase of the rate coefficient. A comparison of rate coefficients
210 for 2-butanone and 3-methylbutan-2-one reveals this effect, particularly pronounced in OH reactions. The presence
211 of two methyl groups (33DMbutanone) produces a significant decrease in the value of the rate coefficient, that again
212 could be explained by steric hindrance.

213 As can be observed in Table 2, the type of carbonyl group (aldehyde or ketone) also exerts a significant influence
214 on the reactivity. The rate coefficients are generally one or two orders of magnitude higher for the aldehyde reactions
215 compared to the reaction of ketones. The different reactivity of aldehydes and ketones with main atmospheric
216 oxidants has extensively been studied and documented in the literature (McGillen et al., 2020, Mellouki et al., 2015.).
217 The different reactivity observed in the reactions of atmospheric radical with saturated carbonyl compounds that are
218 initiated by hydrogen abstraction, are due to the presence in the carbonyl compound of different types of hydrogens.
219 In the aldehydic compounds there are two types of hydrogens that can be abstracted, the hydrogen directly attached
220 to the carbonyl group (aldehydic hydrogen) and the hydrogen attached to the alkyl group (alkyl hydrogen), while in



221 a ketone only alkyl hydrogens are present. The available kinetic and mechanistic data on the atmospheric degradation
222 indicate that the H atom abstraction from the aldehydic group (–CHO) is more favoured than H atom abstraction
223 from the C–H bonds of the alkyl chain. The rate coefficients obtained in this study for 33DMbutanal and
224 33DMbutanone confirm this argument.

225 On the other hand, it is well known that functional groups exert an activating or deactivating effect on reactivity,
226 depending on the type of groups. The reactivity factors (F(R); R=functional group) associated with the functional
227 group to which a type of carbon is attached (primary (k_{prim}), secondary (k_{sec}) or tertiary (k_{ter})) can be quantified using
228 the experimental kinetic database available in the literature. Consequently, rate coefficients for the reactions of
229 33DMbutanal and 33DMbutanone with Cl atoms and OH and NO₃ radicals have been estimated with the SAR
230 (Structure-Activity Relationship) predictive method (Calvert et al., 2011, Kerdouci et al., 2014, Kwok and Atkinson,
231 1995). In the case of the two carbonyl compounds of this work, the only possibility of reacting is the abstraction of
232 one hydrogen atom due to the absence of double bonds. The global abstraction rate coefficients can be calculated as
233 $k_{\text{abs}} = 3(k_{\text{prim}}F(\text{C})) + k_{\text{sec}}F(\text{C})F(-\text{CHO}) + k_{-\text{COH}}F(\text{CH}_2)$ for 33DMbutanal and $k_{\text{abs}} =$
234 $3(k_{\text{prim}}F(-\text{CR}_2\text{CO}-)) + (k_{\text{prim}}F(-\text{CO}-))$ for 33DMbutanone.

235 The rate coefficients (in cm³ molecule⁻¹ s⁻¹) and factors used to obtain the estimated rate coefficients for
236 33DMbutanal and 33DMbutanone with Cl atoms are: $k_{\text{prim}}=2.84 \times 10^{-11}$, $k_{\text{sec}}=8.95 \times 10^{-11}$, $k_{-\text{COH}}=5.13 \times 10^{-11}$, $F(\text{C})=0.79$
237 proposed by Calvert et al., 2011, $F(-\text{CHO})=0.4$ proposed by Carter et al 2021, $F(-\text{CR}_2\text{CO}-)=0.563$ and $F(-\text{CO})=0.037$
238 proposed by Farrugia et al., 2015. Therefore, the estimated rate coefficient for Cl reaction have been 1.36×10^{-10} and
239 0.49×10^{-10} cm³ molecule⁻¹ s⁻¹ for 33DMbutanal and 33DM-2-butanone respectively. In the case of OH reactions the
240 rate coefficients have been estimated using the EPI (Estimation Programs Interface) Suite™, (US EPA), specifically
241 the AOPWIN™. The rate coefficients estimated have been $k_{\text{estimated}}=22.12 \times 10^{-12}$ for 33DMbutanal and
242 $k_{\text{estimated}}=1.69 \times 10^{-12}$ for 33DM-2-butanone. For the reaction of NO₃ radical only the estimated rate coefficient for
243 33DMbutanal have been done obtaining a $k_{\text{estimated}}=2 \times 10^{-14}$ cm³ molecule⁻¹ s⁻¹ using the data of Kerdouci et al.,
244 (2014). In all cases the estimated rate coefficients are very similar to the experimental values, indicating that the
245 reactivity factor used for the estimations are well established. Reaction product studies and theoretical calculations
246 of these reactions will help confirm the arguments presented above.

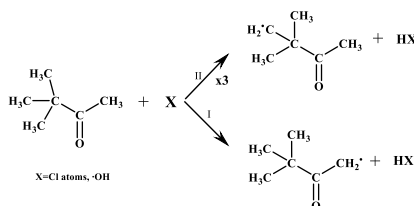
247 3.2 Products study and Mechanisms of reaction

248 The products of the reactions of 33DMbutanal and 33DMbutanone with Cl atoms have been studied in the presence
249 and in the absence of NO to evaluate different atmospheric conditions. In addition, the products of the reaction of
250 33DMbutanal with OH and NO₃ radical and 33DMbutanone with OH radicals have also been studied. All these
251 reactions have been carried out using the experimental systems described above.

252 Based on the principles of tropospheric reactivity (Atkinson, 2007, Finlayson-Pitts and Pitts 2000) and in the case
253 of 33DMbutanal in a previous products study with OH (Aschmann et al. 2010), a complete reaction mechanism has
254 been proposed for both carbonyls to facilitate the identification of the products. The Scheme 1S and 2S
255 (supplementary information) show these reaction mechanisms.



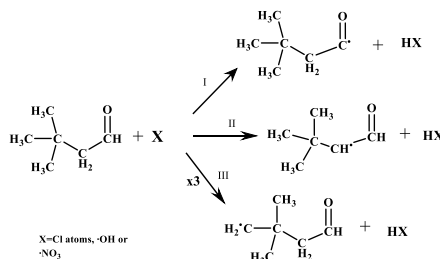
256 In the proposed mechanism for the reactions of 33DMbutanone (Scheme 1S), the initial attack by the oxidant can
 257 occur at the -CH₃ in the α-position with respect to the carbonyl (channel I) or at any of the -CH₃ of the tert-butyl
 258 group (channel II).



259

260 According to the SAR predictions the H-abstraction in the -CH₃ of the tert-butyl group is the main channel, for the
 261 reaction with both oxidants (~ 98 % for Cl atoms and ~ 94% for OH radicals, see Table 1S).

262 In the proposed mechanism of the reactions of 33DMbutanal (Scheme 2S), the initial attack can take place in three
 263 different groups: -CHO (channel I) -CH₂- (channel II) and -CH₃ (channel III) from tert-butyl group.



264

265 Aschman et al., (2010) proposed the reaction in the -CHO group as the mayor initial channel of this compound
 266 with OH radicals. However, according to the SAR predictions used in this work, the main initial attack depends on
 267 the type of oxidants. Therefore, for the reaction with Cl atoms the main initial attack would take place in the -CH₃
 268 (~ 49%) followed by -CHO (~ 30%) and lastly the -CH₂- group with ~21%. For the reaction of 33DMbutanal with
 269 NO₃ radical the main initial attack would take place in the CHO (~ 63%) followed by -CH₂-(~37%). And for OH
 270 reactions the main initial attack of the radical would take place in the -CHO (~ 94%) followed by -CH₂- (~ 4%) and
 271 lastly the -CH₃ (~2%). Note that the percentage of -CH₃ corresponds to three times the % of channel III (see Table
 272 1S).

273 It is well established (Atkinson, 2007) that alkyl radicals, formed in the initial step of these reactions, rapidly react
 274 with O₂ to generate the corresponding peroxyradical (RO₂·). These RO₂ radicals can undergo various pathways (see
 275 Schemes 1S and 2S). In the absence of NO, peroxyradicals primarily undergo two self-reaction processes: one
 276 leading to the formation of alkoxyradicals (RO₂· + RO₂· → 2RO· + O₂), and the other producing neutral compounds,
 277 such as hydroxy compounds and carbonyl compounds (RO₂· + RO₂· → hydroxy compound + carbonyl compound
 278 + O₂). Another significant process is the reaction of RO₂ with OH radicals, the likelihood of which depends on the
 279 size and structure of the alkyl group (R) (Berndt et al., 2018; Bottorff et al., 2023; Fittschen, 2019).

280 In the presence of NO, the RO₂ radical may react to form alkoxyradicals and NO₂ (RO₂· + NO· → RO· + NO₂) or
 281 nitrated compounds (RONO₂), and in presence of large concentration of NO₂, RO₂ generates peroxy-nitrated



282 compounds (ROONO₂) (pathway less favoured). Under typical tropospheric conditions, alkoxyradicals can react
283 with oxygen, undergo unimolecular decomposition, or isomerize (Atkinson, 2007). The reaction of RO· radicals
284 with O₂ is only possible if the carbon atom bearing the radical contains at least one hydrogen atom (Atkinson, 2007).
285 Additionally, in the presence of NO and NO₂, alkoxyradicals can also form nitrated compounds.

286 In an effort to establish the main reaction paths for the reactions studied in this work, the rate coefficient for
287 unimolecular decomposition and isomerization have been estimated following the method outlined by Vereecken
288 and Peeters (2009, 2010). In the case of 33DMbutanone, the rate coefficients estimated for the unimolecular
289 isomerization of the initial alkoxyradical formed in both pathways were found to be at least one order of magnitude
290 lower than the estimated rate coefficients for the decomposition of the same alkoxyradical. Consequently, the
291 reaction products generated from isomerization channel will not be important. In channel II, the estimated rate
292 coefficient of the decomposition process to obtain acetone has been $1.7 \times 10^{12} \text{ s}^{-1}$, that is much higher than the
293 estimated rate coefficient to obtain butane-2,3-dione ($6 \times 10^3 \text{ s}^{-1}$). In the case of 33DMbutanal there is one possibility
294 of isomerization in channel III where the H-atom implied come from the aldehydic group. However, based on the
295 estimated rate coefficients, the rate coefficient for decomposition is four times higher than that for the isomerization
296 process.

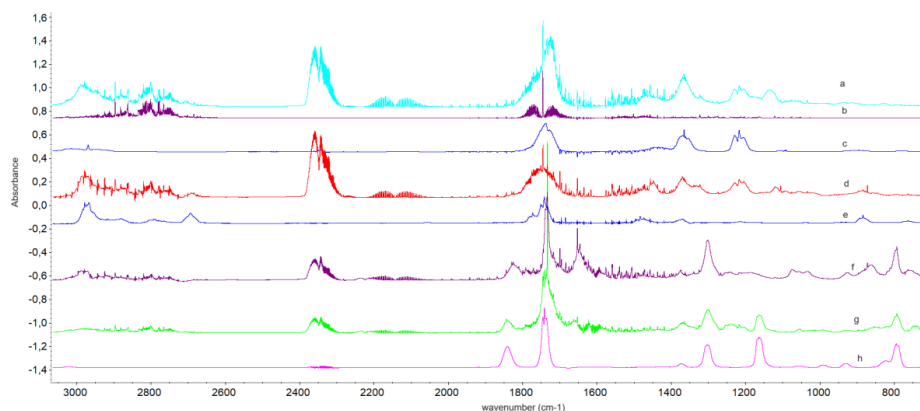
297 Based on the general mechanism proposed in Scheme 1S for 33DMbutanone and Scheme 2S for 33DMbutanal
298 respectively, the formation of the expected products have been investigated using two analytical techniques. Also,
299 the influence of the presence or absence of NO in the reaction of these two carbonyls with Cl atoms has been
300 evaluated.

301 3.2.1 FTIR experiments

302 The procedure followed to analyse the FTIR spectra have been described in previous works (Aranda et al., 2020,
303 Aranda et al., 2024, Colmenar et al., 2108, 2020a, 2020b). Therefore, only the main results will be indicated.

304 The residual IR spectra of the reaction products, obtained after subtracting the spectra of all known compounds
305 (33DMbutanone, 33DMbutanal, HCl, NO, NO₂, CH₃NO₂, N₂O₅, HNO₃, HNO₂, etc.), were compared with IR spectra
306 of commercial samples or database spectra (Eurochamp 2020 database <https://data.eurochamp.org/data-access/spectra/>) last access: 9 July 2024). The identified and quantified reaction products were acetone
308 (CH₃C(O)CH₃) and formaldehyde (HCHO) for all reactions (except to 33DMbutanal with NO₃); 2,2-
309 dimethylpropanal ((22DM)propanal, (CH₃)₃CCHO)) for the reactions of 33DMbutanal with Cl atoms; and nitrated
310 compounds in those reactions carried out in presence of NO and/or NO₂. The nitrated compounds were attributed to
311 alkoxy nitrates (RONO₂ ~1663, 1284, 853 cm⁻¹) and peroxy nitrates (ROONO₂ ~1718, 1300 and 793 cm⁻¹)
312 (Finlayson-Pitts and Pitts, 2000). A peroxy carbonyl nitrates as PeroxyAcetyl Nitrate (PAN, CH₃C(O)OONO₂
313 ~1830, 1300 and 793 cm⁻¹) was identified and quantified in reactions of 33DMbutanone + Cl conducted in the
314 presence of NO after 3-5 minutes of reaction time. Figure 2 shows an example of residual spectra from the reactions
315 of 33DMbutanone and 33DMbutanal with Cl atoms in the absence and presence of NO. The figure includes reference
316 spectra to corroborate the formation of these compounds.

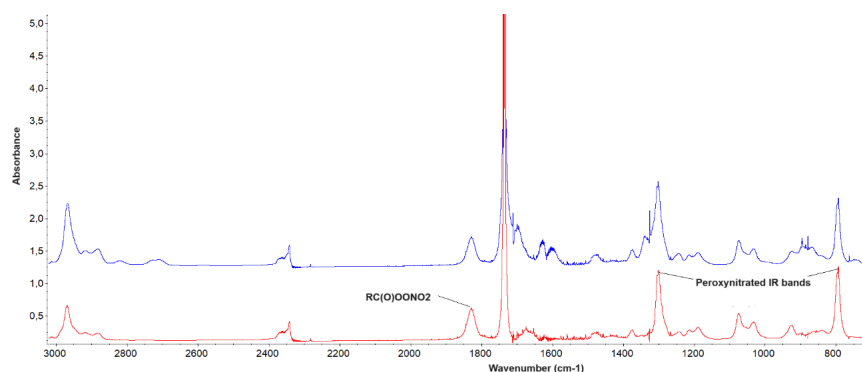
317



318

319 Figure 2. Residual FTIR spectra for the reactions of: 33DMbutanone with Cl in the absence of NO at 21 min (a) and
320 in the presence of NO at 21 min (g), 33DMbutanal with Cl atoms in the absence of NO at 18 min (d) and in the
321 presence of NO at 18 min (f) 64 % of the conversion and a 29% respectively. Reference IR spectrum of HCHO (b)
322 acetone (c) (commercial sample), 22DMpropanal (e) and PAN (h). The spectra have been shifted for clarity.

323 For the reactions of 33DMbutanal with NO₃, nitrated bands attributed to alkoxy nitrates, peroxy nitrates and
324 peroxy carbonyl nitrates are clearly observed. The peroxy carbonyl nitrates could correspond to peroxy-3,3-
325 dimethylbutyryl nitrate ((CH₃)₃CCH₂C(O)OONO₂) that is formed due to the large amount of NO₂ presents in the
326 reaction mixture from the initial time. Figure 3 shows the characteristic IR absorption bands of nitrated compounds
327 formed in the reaction of 33DMbutanal with NO₃.



328

329 Figure 3. FTIR spectrum of the reaction of 33DMbutanal (~25% of conversion) with NO₃ radical (upper). FTIR
330 residual spectra (assigned to peroxy-3,3-dimethylbutyryl nitrate) after elimination of N₂O₅, HNO₃, 33DMbutanal
331 and NO₂ (lower).

332 It is important to note that for the reactions of 33DMbutanal with Cl atoms (in the presence of NO) and with OH
333 radical at large reaction times, a nitrated compound, as observed in the NO₃ reaction, has been detected. Additionally,
334 IR bands of N₂O₅ (precursor of NO₃) has been observed in the reaction with Cl atoms as consequence of the reaction
335 of O₃ + NO₂. This last result indicates the formation of ozone in the degradation process of
336 33DMbutanone/33DMbutanal in the presence of radiation and NO₂.



337 Figure 2S shows IR spectra of the nitrated compounds together with N₂O₅ reference spectrum. The IR bands of the
338 nitrated compounds show great absorbance in the case of Cl reaction compared to the OH reactions. This fact could
339 be due to an additional contribution from the 33DMbutanal reaction with NO₃. On the other hand, 22DMpropanal
340 has not been observed in the reactions of 33DMbutanal with OH and NO₃ radicals, probably due to the overlapping
341 of their characteristic IR bands with the ones of nitrated compounds.

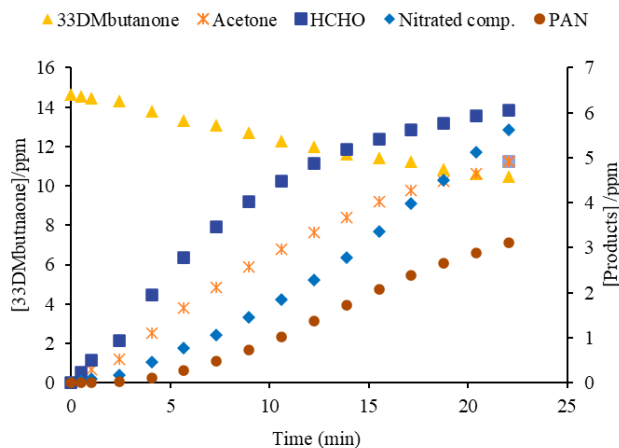
342 To evaluate the amount of nitrated compounds formed in the reactions studied with Cl atoms in the presence of NO,
343 and in the 33DMbutanal reaction with NO₃ an estimation has been made using the average integrated absorption
344 coefficient of 1.2×10^{-17} cm molecule⁻¹ corresponding to the IR range 1250-1330 cm⁻¹ for similar compounds
345 (Tuazon and Atkinson, 1990). In the reaction of 33DMbutanal and 33DMbutanone with OH radicals, the yield of
346 nitrated compounds was not estimated, because there is an additional contribution due to the precursor used
347 (methylnitrite). For PAN quantification in the reaction of 33DMbutanone with Cl in the presence of NO, the
348 reference spectrum (Eurochamp 2020 database, <https://data.eurochamp.org/data-access/spectra/>) last access:
349 September 2024) has been used.

350 The time-concentration profiles of the quantified products formed, and the consumption of the carbonyl reactant
351 have been represented in Figure 4.

352

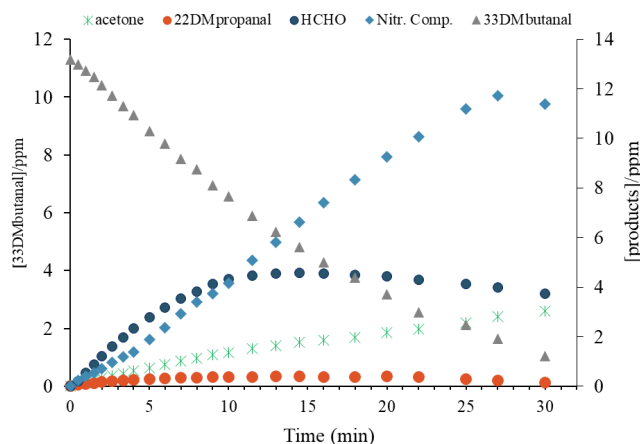


353 (a)



354

355 (b)



356

357 Figure 4. Time-concentration profiles of the products formed, and the carbonyl reacted for the reaction of (a)
358 33DMbutanone and (b) 33DMbutanal with Cl atoms in the presence of NO. For 33DMbutanone + Cl + NO, the
359 nitrated compounds profiles are the total nitrated compounds (alcoxy, peroxy and PAN).

360 For the reaction of 33DMbutanone with Cl atoms, the trends of acetone and HCHO indicate that they are primary
361 products, although the concentration of HCHO starts to decrease at 20 min of reaction, possibly due to secondary
362 chemical reactions. The profile of nitrated compounds, especially PAN, shows a significant increase after 5 minutes
363 of reaction. In the case of the reaction of 33DMbutanal with Cl atoms, all trends (for acetone, HCHO, 22DMpropanal
364 and nitrated compounds) suggest that they are primary products in the early stages. However, 22DMpropanal and
365 HCHO seem to undergo further reactions due to secondary chemistry, while the concentrations of acetone and
366 nitrated compounds increase more than expected, likely due to contributions from other sources (Figures 3S-5S).
367 For the nitrated compounds, a change in the trend is observed around 2 minutes, likely due to the formation of
368 nitrated peroxy carbonyl compounds as a result of the presence of NO₂ in the reaction mixture. The profile of nitrated



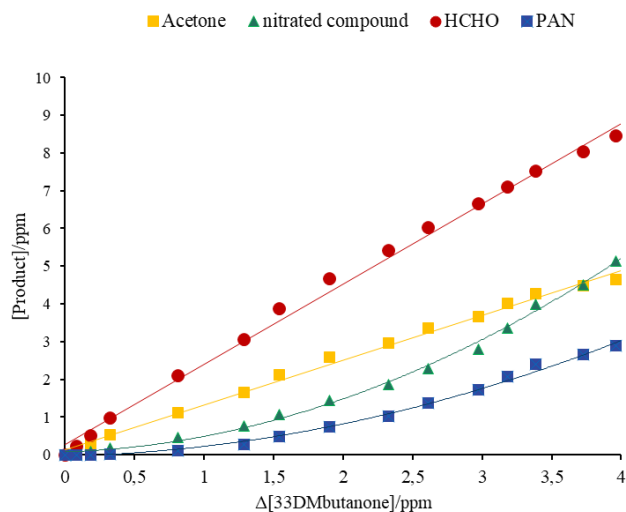
369 compounds from the reaction of 33DMbutanal with NO_3 shows an increase from the initial of the reaction (see
370 Figure 4S), due to the presence of NO_2 in the reaction medium from the beginning.

371 The yields for primary products have been calculated from the slopes of the plots of the concentration of the products
372 formed against the variation in the carbonyl reactant consumed using the first data of the reactions to avoid secondary
373 chemistry contributions. In some cases, the yields have been difficult to obtain due to the overlapping of IR bands
374 with other unidentified products. In these cases, in which the concentration of the compounds that seems to react
375 with the main oxidant (such as 22DMpropanal and HCHO) the yields have been recalculated using the formalism
376 published by Tuazon et al., 1986. Figure 5 showed an example of yield plots for the reactions of 33DMbutanal with
377 Cl atoms in the absence and the presence of NO. The yield of PAN formed in the reaction of 33DMbutanone with
378 Cl atoms in the presence of NO has been estimated from the slopes of the plots, where the data show a linear
379 behavior, corresponding to a $\Delta[3,3\text{DMbutanone}]$ of approximately 1.5 ppm (see Figure 5a).

380

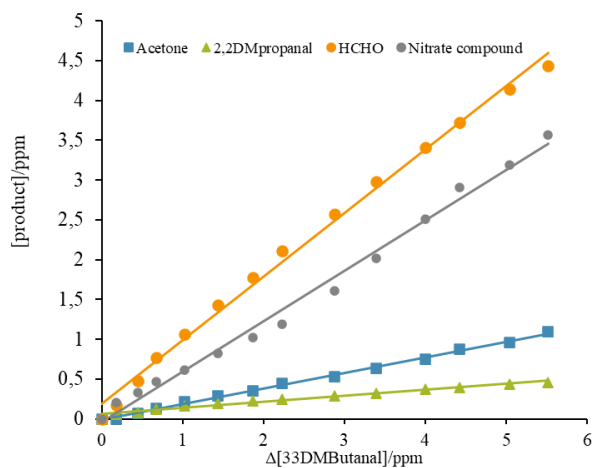


381 (a)



382

383 (b)



384

385 Figure 5. Plots of the reaction product formed versus the consumption of the reactant in the reaction of (a)
386 33DMbutanone + Cl + NO and (b) 33DMbutanal + Cl + NO.

387 The Figures 6S and 7S of supplementary material show the yield plots for the reactions of 33DMbutanone and
388 33DMbutanal with Cl atoms and 33DMbutanone with OH in the absence of NO respectively.

389 A summary of the estimated yields of reaction products, identified and quantified through FTIR analysis, is presented
390 in Table 3 for the reaction of 33DMbutanone + Cl, Cl + NO and + OH radical. Table 4 shows the results for the



391 reactions of 33DMbutanal + Cl; Cl + NO, OH and NO₃ radical. Table 3. Estimated yields (%) of reaction products
 392 identified with FTIR analysis and the reaction products tentatively assigned from SPME/GC-TOFMS analysis in
 393 the reactions of 33DMbutanone with Cl atoms and OH radical in the absence and in the presence of NO.

394 Table 3. Estimated yields (%) of reaction products identified with FTIR analysis and the reaction products tentatively
 395 assigned from SPME/GC-TOFMS analysis in the reactions of 33DMbutanone with Cl atoms and OH radical in the
 396 absence and in the presence of NO.

Reaction	FTIR				GC-TOFMS	
	Yield acetone (%)±2σ	Yield HCHO ^{a,b} (%)±2σ	Yield nitrated comp. (%)±2σ	Yield PAN (%)±2σ	t _r min	Reaction Product
33DMbutanone + Cl	65.0±1.1	153.3±7.0			2.2	Acetone
	65.9±1.8	178.1±4.1			2.87	Hydroxyacetone
	69.0±1.3	174.7±3.6			7.03	Hydroxy-2,3-butanodione
Average	66.6±4.2	168.7±30.0				
Total carbon^{c, d} (%)	61				8.28	2,2DM3-oxo-butanal
					10.26	4-hydroxy-3,3-DM2butanone
33DMbutanone + Cl + NO	123.2±3.2	212.4±7.4	59.2±1.9	101.0±7.0	2*	Acetone
	111.2±6.3	195.4±5.8	56.6±6.6	112.9±18.4	5.59	Peroxyacetylnitrate (PAN)
	137.4±11.0	199.9±11.5	66.9±6.1	95.5±44.2	6.81*(7.03) ⁽¹⁾	Hydroxy-2,3-butanodione
	Average	124.0±26.2	202.6±17.6	60.9±10.7	103.1±8.8	8.01*(8.28)
Total carbon^{c, d} (%)	95.6				9.04	2,2-dimethyl-3-propyl-oxynitrite
					9.68	Nitrated compound
					14.57	Nitrated compound
33DMbutanone + OH ^e	31.4±2.0	59.5±2.4			-	-
	31.5±1.0	68.2±3.8				
	34.1±1.6	73.5±4.2				
Average	32.3±3.0	67±14				
Total carbon^{c, d} (%)	28					
33DMbutanone + OH+NO ^f	121.1±6.7	-	-		2.01	Acetone
	161.9±19.7	-	-		2.55	Nitrated compound
	89.2±6.4	-	-		9.04	2,2-dimethyl-3-propyl-oxynitrite
Average^g	93.0±72.8	-	-		14.62	Nitrated compound
Total carbon^{c, d} (%)	47					

397 ^aYields have been estimated using the reference IR spectra from the Eurochamp database (Rodenas et al., 2017). ^bThe rate
 398 coefficient used to correct the concentration of formaldehyde has been $k_{Cl}=7.2 \times 10^{-11} \text{ cm}^3 \text{ molecule}^{-1} \text{ s}^{-1}$ from IUPAC(2017).^c
 399 $Total\ carbon = \sum_i \frac{n^o\ of\ carbon\ of\ product_i}{n^o\ of\ carbon\ of\ 33dmbutanone} \times molar\ yield_i$. ^d Nitrated compounds have not been accounted for total
 400 carbons. ^eOnly FTIR experiments using H₂O₂ as OH radical precursor. ^fExperiments using methyl nitrite as OH radical precursor.
 401 ^gThe acetone yield must be taken with caution due to interference with IR bands of methyl nitrite. The yield of HCHO and
 402 nitrated compounds for the reaction of 33DMbutanal with OH radical has not been determined, as there is a significant
 403 contribution from other sources such as the precursor used to generate the OH radical (which is a nitrated compound, methyl
 404 nitrite) and its degradation (which generates methyl nitrate and formaldehyde). ⁽¹⁾ Little Peaks *GC-TOFMS experiments. The

<https://doi.org/10.5194/egusphere-2024-3241>

Preprint. Discussion started: 22 October 2024

© Author(s) 2024. CC BY 4.0 License.



405 retention time shorter than Cl+NO and OH experiment due to the use of a different chromatographic column. The positive
406 identification and quantification were not possible due to the scarce of commercial standards.

407



408 Table 4. Estimated yields (%) for reaction products formed in the reactions of 33DMbutanal with Cl atoms in the
 409 absence and in the presence of NO and with NO₃ and OH radical using FTIR and the product identify in the
 410 qualitative analysis using GC-TOFMS.

Reaction	FTIR				GC-TOFMS		
	Yield 22DMpropanal ^a (%)±2σ	Yield acetone (%)±2σ	Yield HCHO ^{b,c} (%)±2σ	Yield Nitrated comp. (%)±2σ	t _r min	Reaction Product	
33DMbutanal + Cl	28.4±0.4	31.1±0.6	37.4±0.3	-	2.2	Acetone	
	29.6±0.3	26.8±0.4	38.5±0.4	-	2.65	Hydroxyacetone	
	29.9±2.0	27.5±0.3	40.5±1.0	-	3.42	22DMpropanal	
	Average	29.3±0.7	28.5±2.4	38.8±1.5	-	5.82	22DMpropanol
Total carbon^d (%)					8.23	22DMbutanodial/22DM- propanoic acid**	
					9.57	33DMbutanoic acid	
					13.25	22DMtetrahydrofuranone	
					15.78	4-hydroxi-3,3DMbutanal or (2,3-dihydro-4,4- DMfuran)	
					16.14	3-hydroxy-22-DMpropanal	
					20.90	22dimethylpropane-1,3diol	
		45					
33DMbutanal + Cl + NO	12.8±2.6	20.3±0.6	83.3±1.9	52.1±3.1	2.2	Acetone	
	7.7±0.2	20.8±0.3	89.2±1.4	50.3±3.2	3.41	22DMpropanal	
	7.6±0.2	22.4±1.0	95.3±3.1	52.5±2.0	5.82	22DMpropanol	
	Average	9.4±3.0	21.1±1.1	89.3±6.0	51.6±1.2	6.97	peroxy-3,3- dimethylbutyryl nitrate
					8.26	33DM-oxo-butanal/22DM- propanoic acid**	
Total carbon^{d,e} (%)					9.58	33DMbutanoic acid	
					13.25	2,2-DMtetrahydrofuranone	
					16.16	3-hydroxy-2,2DMpropanal	
		33.2					
33DMbutanal + NO ₃	Not observed	Not observed	Not observed	100	2	Acetone	
					3.08*(3.42)	2,2DMpropanal	
					5.47*(5.82)	2,2DMpropanol	
					6.68*(6.97)	peroxy-3,3- dimethylbutyryl nitrate	
					7.15	Nitrated compound	
					7.88*(8.23)	33DM-oxo-butanal /22DMpropanoic acid**	
33DMbutanal + OH	Not observed ⁽¹⁾	24.9±0.8	-	-	8.94 (9.56)	33DMbutanoic acid	
		34.6±1.0	-	-	2	Acetone	
		37.1±0.7	-	-	7.16	Nitrated compound	
Average		32.2±6.4			8.92*(9.56)	33DMbutanoic acid	
Total carbon^d (%)		16.1					

411 ^aThe rate coefficient used to correct the concentration of 22DMpropanal has been $k_{Cl} = 1.42 \times 10^{-10} \text{ cm}^3 \text{ molecule}^{-1} \text{ s}^{-1}$ from Calvert
 412 et al., 2011. ^b Yields has been estimated using the reference IR spectra from the Eurochamp database (Rodenas et al., 2017). ^cThe
 413 rate coefficient used to correct the concentration of formaldehyde has been $k_{Cl} = 7.2 \times 10^{-11} \text{ cm}^3 \text{ molecule}^{-1} \text{ s}^{-1}$ from IUPAC(2017).^d
 414 $Total\ carbon = \sum_i \frac{n^o\ of\ carbon\ of\ product_i}{n^o\ of\ carbon\ of\ 33dmbutanal} \times molar\ yield_i$. ^e Nitrated compounds have not been accounted for. ⁽¹⁾ Probable
 415 interference with IR bands of nitrated compounds. The yield of HCHO and nitrated compounds has not been determined, as there



416 is a significant contribution from sources other than the main reaction, such as the precursor used to generate the OH radical
417 (which is a nitrated compound, methyl nitrite) and its degradation (which generates methyl nitrate and formaldehyde). *GC-
418 TOFMS experiments. Retention time shorter than Cl experiments due to the use of a different chromatographic column. The
419 positive identification and quantification were not possible to scarce of commercial standards. Ony 22DMpropanal was confirmed
420 with standard. **Secondary reaction product

421 As shown in Tables 3 and 4, the range of total carbon recovered is less than 100%. Only in the case of the reaction
422 of 33DMbutanone with Cl atoms in the presence of NO the total carbon is 95% (not accounting for nitrated
423 compounds), but it is important to note that the residual FTIR spectra (see Figure 8S) indicate the presence of other
424 compounds that are not accounted for total carbon. The residual spectra magnified (see Figure 9S) shows IR
425 absorption bands that can be assigned to reaction products proposed in the general Scheme 1S as formic acid and
426 hydroxyacetone. On the other hand, it is interesting to note that in the residual spectra for the reaction of
427 33DMbutanal with the three oxidants, showed in Figure 10S, some IR absorption bands appear at the same
428 wavenumber indicating common reaction products.

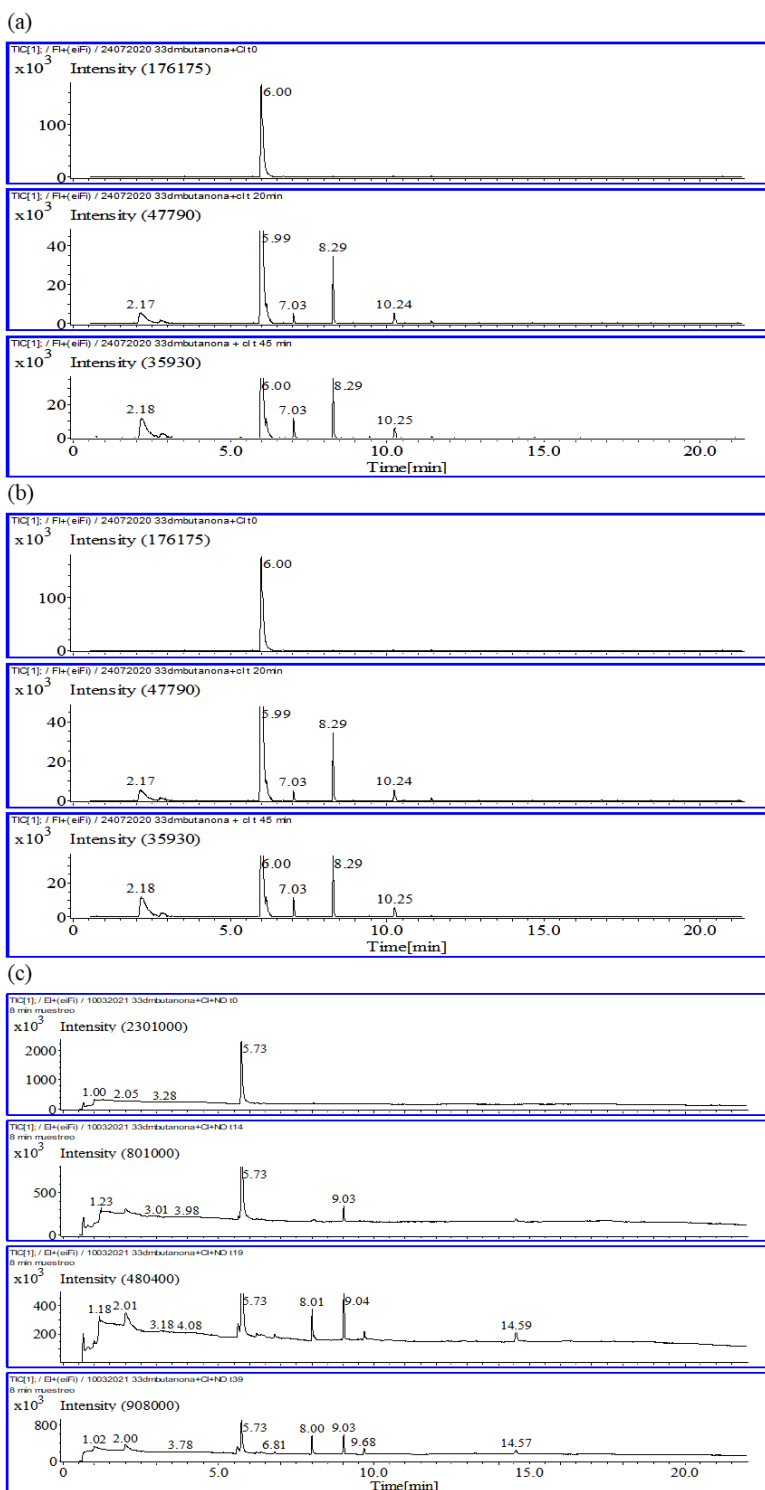
429 Gas chromatography coupled with a time-of-flight mass spectrometer (GC-MSTOF) using EI and/or FI ionization
430 mode has been employed as a complementary technique to FTIR to identify more reaction products or to confirm
431 those detected by FTIR. The yields should be considered with caution due to potential systematic errors during the
432 quantification analysis.

433 3.2.2 SPME/GC-TOFMS experiments

434 The SPME/GC-TOFMS chromatograms in Electron ionization mode (EI) collected at different reaction times for
435 the studied reaction, show peaks at different retention times whose areas increase with the reaction time, indicating
436 that they correspond to reaction products. (Figure 11S). Due to the characteristic of SPME sampling method, only a
437 qualitative analysis was possible.

438 For the reaction of 33DMbutanone with Cl atoms in the presence and the absence of NO, also GC-MS analysis using
439 Field Ionization was carried out. The FI mass spectrum helps to establish the identification of reaction products.
440 Figure 6 shows an example of the SPME/GC-TOFMS chromatograms collected in FI and EI mode for the reaction
441 of 33DMbutanone with Cl.

442





444 Figure 6. Example of the SPME/GC-TOFMS chromatograms for the reaction of 33DMbutanone + Cl atoms (a) in
445 the absence of NO and FI mode, (b) in the presence of NO and FI mode and (c) in presence of NO and EI mode.

446 It can be observed that the FI chromatograms in the absence of NO (a) present more peaks than the corresponding
447 ones in the presence of NO (b), with only one peak being common ($t_r = 8.29$ min). This indicates that the presence
448 of NO influences the reaction mechanism. In the case of the chromatograms obtained under the same reaction
449 conditions but with different ionization modes ((b) and (c) chromatograms), a different number of peaks also is
450 observed, probably because some reaction products were not ionized with FI (peaks at $t_r=9.68$ and 14.57).
451 Additionally, the peak in chromatogram (a) and (b) of 33DMbutanone appears at shorter retention times than in
452 chromatogram (c), due to the use of a different chromatographic column. Taking into account this, the peaks at
453 $t_r=2.24$; 6 ; and 8.29 min, showed in chromatograms (b) correspond with the peaks at $t_r=2$; 5.73 ; 8.0 and 9.03 min in
454 chromatograms (c).

455 The mass spectrum of each peak was analysed using the NIST database of GC-MS or comparing with the mass
456 spectrum of the commercial sample. In some cases, the positive identification with high percentage of similitude
457 index were obtained but in other cases, only a tentative assignation was possible based on profile of fragments m/z
458 generated and the reaction products expected according to the schemes 1S and 2S proposed. In those cases, in which
459 FI spectrum could be obtained, the assignation was made based on fragment m/z of molecular weight. All
460 chromatograms collected in EI mode present a little peak that appear together with the peak of air, that could
461 correspond to acetone. In order to confirm the presence of acetone to this retention time (~ 2 min) a chromatogram
462 has been created using a specific tool of the software of mass spectrometer. For that, in the software it is specified
463 the desired m/z (58 m/z for acetone) and then the chromatogram is generated, displaying the ion intensity versus
464 time, with peaks representing the compounds that correspond to the specified m/z . With this tool the experimental
465 chromatograms have been modified in for a better analysis of all chromatographic peaks. Prior to the mass spectra
466 analysis, it was verified that the experimental and generated chromatograms were identical. In the supplementary
467 material, the GC-TOFMS chromatograms generated with this tool for all reactions are compiled (Figures 12S-16S).

468 The mass spectra of all chromatographic peaks are presented in Tables 2S-3S for the reactions of 33DMbutanone
469 and 33DMbutanal, respectively. An assignment of the reaction products corresponding to each peak has been made,
470 taking into account schemes 1S, 2S and the results of FTIR experiments. However, due to the unavailability of
471 commercial samples, the formation of some product proposed could not positively confirmed. Only in the reaction
472 of 33DMbutanal, the injection of a real sample of 22DMpropanal, allowed the confirmation of this product assigned
473 to a peak at $t_r = 3.08/3.41$ minutes.

474 The SPME/GC-TOFMS experiments show the formation of the main compounds quantified in the FTIR
475 experiments, such as acetone and 2,2-dimethylpropanal (22DMpropanal) in the case of the 33DMbutanal reactions.
476 Due to the SPME sampling procedure, formaldehyde could not be detected. The formation of other organic
477 compounds, generally multifunctional of varying alkyl chain lengths, (hydroxycarbonyls, oxocarbonyls, hydroxy-
478 oxo-carbonyls, organic acids) is observed. These compounds could correspond to the unidentified compounds in the
479 FTIR spectra.

480 Next a discussion of the results on reaction products with both analytical techniques for each of the compounds
481 studied is presented.



482 3.2.2.1 33DMbutanone reaction products

483 In the SPME/GC-TOFMS chromatograms for the reactions of 33DMbutanone (Figures 6, 12S) can see that the
484 number of peaks and therefore the reaction products generated is different. Based on the retention times and mass
485 spectra summarized in Table 2S, similar compounds seem to be formed in these reactions.

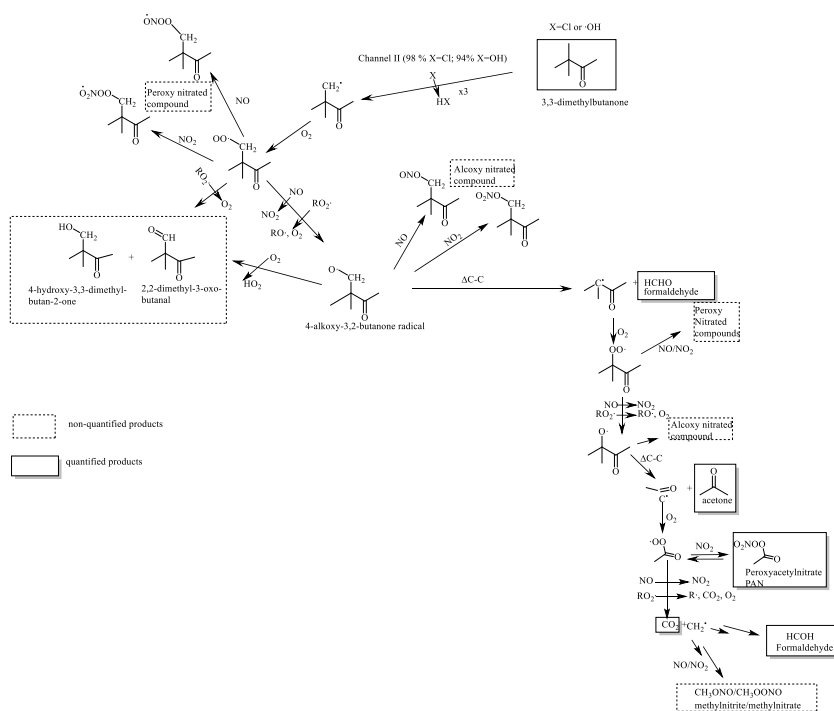
486 As shown in Table 3, the percentage of acetone and formaldehyde in the reactions with Cl and OH in the presence
487 of NO is higher than in experiments without NO. This indicates that, in the presence of NO, the formation of the
488 alkoxy radical by reaction of the peroxy radical (RO₂·) with NO is favored, compared to the formation of this same
489 alkoxy radical by self-reaction of RO₂. Additionally, these alkoxy radicals are chemically activated and undergo
490 'prompt' decomposition to form acetone, in contrast to alkoxy radicals formed by the self-reaction of RO₂, which are
491 more thermally stabilized (Atkinson et al., 2007). In the reactions of 33DMbutanone in the absence of NO, the
492 percentage of acetone is lower in the OH reaction than Cl reaction, which could be explained by the possible reaction
493 of RO₂ with OH radical present in the reaction medium, to form RO₂OH rather than RO₂ reacting with itself to yield
494 two alkoxy radicals. The IR band observed at ~1800 cm⁻¹ for 33DMbutanone + Cl reaction could correspond with
495 the stretching vibration of the C=O (carbonyl) bond in acyl chloride. This compound can be formed by the reaction
496 of RO₂ with Cl₂ or Cl atoms (Ren et al., 2018). In the Cl reaction without NO, the identification of a product with a
497 molecular mass of m/z=116 (at t_r=10.26 min), assigned to 4-hydroxy-3,3-dimethyl-2-butanone (see Table 2S), is
498 explained by the self-reaction of two RO₂ radicals, leading to the formation of two molecules. In this case, the co-
499 product molecule to 4-hydroxy-3,3-dimethyl-2-butanone would correspond to a compound with a molecular weight
500 of m/z=114 (at t_r=8.28), assigned to 2,2-dimethyl-2-oxo-butanal. This compound is also observed in the Cl reaction
501 in the presence of NO, formed by the reaction of the alkoxy radical with O₂. The peak at t_r=2.55 min with a mass of
502 m/z=72.08 (Table 2S), assigned to hydroxyacetone, the peak at t_r=7.03 min with a molecular mass of m/z=102,
503 assigned to 1-hydroxybutan-2,3-dione, and the IR absorption band at 1105.42 cm⁻¹ (see Figure 10S), characteristic
504 of formic acid, indicate that the alkoxy radical also undergoes different isomerization processes.

505 The reaction of 33DMbutanone with Cl and OH in the presence of NO (at short times) and NO₂ (at long times) leads
506 to the formation of chromatographic peaks at t_r=5.59, 9.04, 9.68, and 14.62 min for the Cl reaction, and t_r=2.55,
507 9.04, and 14.62 min for the OH reaction, which have been assigned to nitrated compounds (also observed in the
508 FTIR experiments). Specifically, the peak at 5.59 minutes has been assigned to peroxyacetyl nitrate (PAN).
509 Additionally, based on the IR bands observed in the residual spectra at times less than 5 minutes for the Cl and OH
510 reaction in the presence of NO, other nitrated compounds are assigned as alkoxy nitrates (IR band around 850 cm⁻¹).
511 The formation of PAN can only be explained through the channel II, with the decomposition of the initially formed
512 alkoxy radical (2,2-dimethyl-3-oxobutan-1-yloxy radical). The estimated yield for PAN of 100% indicates that the
513 percentage of Cl attack on the -CH₃ of the tert-butyl group is 100%, a value very close to the 98% estimated by the
514 SAR method for reactions with Cl (see Table 1S).

515 For the reactions with OH, only acetone and formaldehyde have been quantified. These products may come from
516 OH attack on the methyl of the tertiary carbon of 33DMbutanone (channel II) or on the methyl directly attached to
517 the carbonyl group (channel I). Thus, this study cannot confirm that 94% of the reaction proceeds through channel
518 II, as the SAR method suggests. However, considering that the rate coefficient estimated by the SAR method is
519 similar to that obtained in this study, channel II can be considered the main process. From the analysis of the
520 SPME/GC-TOFMS experiments, the proposed reaction products also are listed in Table 3. Based on the kinetic



521 results and the main products obtained in this study, the reaction mechanism showed in Figure 7 is proposed for the
 522 degradation of 33DMbutanone.



523

524 Figure 7. Mechanism proposed by the formation of the main reaction products observed for 33DMbutanone reactions
 525 with Cl atoms and OH radical. The framed products correspond to products identified by FTIR and/or SPME/GC-
 526 TOFMS.

527



528 3.2.2.2 33DMbutanal reaction products

529 In the analysis of SPME/GC-TOFMS chromatograms, the number of peaks observed with appreciable intensity in
530 the reaction of Cl atoms in the presence of NO (10 peaks), in the absence of NO (8 peaks), and in the NO₃ reaction
531 (7 peaks) is greater than in the reaction with OH, where only 3 peaks are observed (see Figures 13S-16S). This fact
532 may be related to the different attack positions of the oxidant when reacting with 33DMbutanal: 3 for the reaction
533 with Cl atoms, 2 for the reaction with the NO₃ radicals, and 1 for the reaction with the OH radicals, as estimated by
534 the SAR method (see Table 1S). Some of these peaks appear at the same retention times, and their mass spectra are
535 very similar (see Table 2S), indicating that they are the same reaction products. Some of these products are also
536 identified in the FTIR analysis (see Table 4), such as acetone ($t_r = 2.2$ min) and 22DMpropanal ($t_r = 3.08$ or 3.43
537 min).

538 It is interesting to note the presence of a common peak for all reactions that appears at 9.56 min (8.95 min in the
539 experiment with a new chromatographic column). The mass spectrum of this peak is assigned to 3,3-
540 dimethylbutanoic acid by the NIST database software, with a similarity index of approximately 84%. This compound
541 cannot be explained by the general scheme proposed (Scheme 2S), which is based on principles of atmospheric
542 reactivity and bibliographic studies of similar compounds (Aschmann et al. 2010, Atkinson et al. 2007). In order to
543 explain the formation of this peak, other pathway was proposed, where the oxy-3,3-dimethylbutyryl radical (channel
544 D), undergoes isomerization. This pathway leads to the formation of 4-oxo-3,3-dimethylbutanoic acid, whose mass
545 spectrum shows a fragmentation pattern very similar to the peak with a t_r of 9.56 min. In order to establish which
546 compound corresponds to this peak and taking into account that 3,3-dimethylbutanoic acid (33DMbutanoic acid) is
547 a commercial compound, a sample of 33DMbutanoic acid was injected into the SPME/GC-TOFMS system. The
548 analysis showed a chromatogram with a peak at approximately 9 minutes, with a mass spectrum (MS) identical to
549 that of the peaks (9.56/8.95 min), which positively confirms the formation of this 3,3-dimethylbutanoic acid in the
550 reactions of 33DMbutanal with atomic Cl and OH and NO₃ radicals (See Figure 17S). The characteristic IR bands
551 of 33DMButanoic acid seem to be present in the FTIR residual spectra obtained for the reaction of 33DMbutanal
552 with Cl atoms (Figure 18S). Recent studies have also detected organic acids from reactions of saturated aldehydes
553 (Asensio et al. 2022, Bo et al. 2022).

554 The remaining chromatographic peaks showed in Figures 13S-16S, have been assigned to reaction products shown
555 in the general Scheme 2S. Table 3S contains all the mass spectra and their assignments. In general, the complete
556 interpretation of mass spectra is complex because the formed products have very similar structures, leading to similar
557 fragmentation patterns. The mass spectrum of chromatographic peaks around 8 min (7.88, 8.23, and 8.26 min) could
558 correspond to several structurally similar products. The injection of a commercial sample of 2,2-dimethylpropanoic
559 acid (22DMpropanoic acid) in the SPME/GC-TOFMS system shows a peak with a retention time of 8 min, whose
560 mass spectrum correspond with the mass spectrum of the peak at 8.23 min observed in the reaction of 33DMbutanal
561 with Cl atoms in the absence of NO. Figure 16S, shows an IR reference spectrum of 22DMpropanoic.

562 As can be seen in Table 3S, some of the proposed reaction products are dicarbonyls or hydroxycarbonyl compounds.
563 The hydroxycarbonyl compounds tend to cyclize to dihydrofurans via acid-catalyzed heterogeneous reactions
564 (Atkinson et al. 2008). For example, 4-hydroxy-3,3DMbutanal ($t_r = 15.78$ min) can cyclize to form 2,3-dihydro-4,4-
565 dimethylfuran. Another cyclization process can occur from an alkoxy carbonyl radical, such as the 4-formyl-2,2-
566 dimethylbutan-1-yloxy radical, leading to the formation of 2,2-dimethyltetrahydrofuran-2-one ($t_r = 13.25$ min).



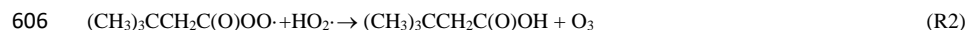
567 The common chromatographic peak at 6.97/6.86 min observed in the Cl + NO and NO₃ reactions has been assigned
568 to a nitrated compound, which could correspond to peroxy-3,3-dimethylbutyl nitrate also detected in the FTIR
569 analysis. The intensity of these peaks is very low, likely because the compound undergoes thermal decomposition
570 in the chromatograph injector. Another small chromatographic peak at 7.15 min observed in the NO₃ and OH radical
571 reactions could correspond to two nitrated compounds with the same retention time: peroxy nitrite (in the case of
572 the OH reaction) and peroxy nitrate (for the NO₃ reaction), according to the characteristic IR bands of peroxy
573 compounds at 793 cm⁻¹ observed in the FTIR spectra (see Figure 10S). Figure 10S also shows an IR band at 810
574 cm⁻¹ for the Cl + NO and OH reactions, which is characteristic of alkoxy nitrated compounds. This common product
575 was not detected in SPME/GC-TOFMS, possibly because it was not adsorbed onto the fiber. In general, SPME/GC-
576 TOFMS is not an effective sampling method for nitrated compounds.

577 Table 4 provides a summary of the reaction products tentatively assigned to the chromatographic peaks observed in
578 the experiments conducted for the reactions of 33DMbutanal with atmospheric oxidants, along with the products
579 identified and quantified using FTIR.

580 Finally, the analysis of the quantified compounds in the FTIR experiment can provide insights into the percentage
581 of each channel or which pathway is favored. Acetone is a reaction product that, according to Scheme 2S, is formed
582 from all channels. However, the similar yields in the Cl, Cl + NO, and OH reactions (28%, 21%, and 32%,
583 respectively) may indicate that acetone is formed from all reactions primarily through channel I. HCHO is also a
584 product formed through all three channels, but the highest yield of formaldehyde, along with the significant decrease
585 of 22DMpropanal obtained in the reaction of Cl in the presence of NO compared to the yields of these compounds
586 for the reaction of chlorine in the absence of NO, could indicate that, in the presence of NO, the reaction of the
587 peroxy species generated in channel I or channel II to form nitrated compounds is favored at the expense of the self-
588 reaction of RO₂.

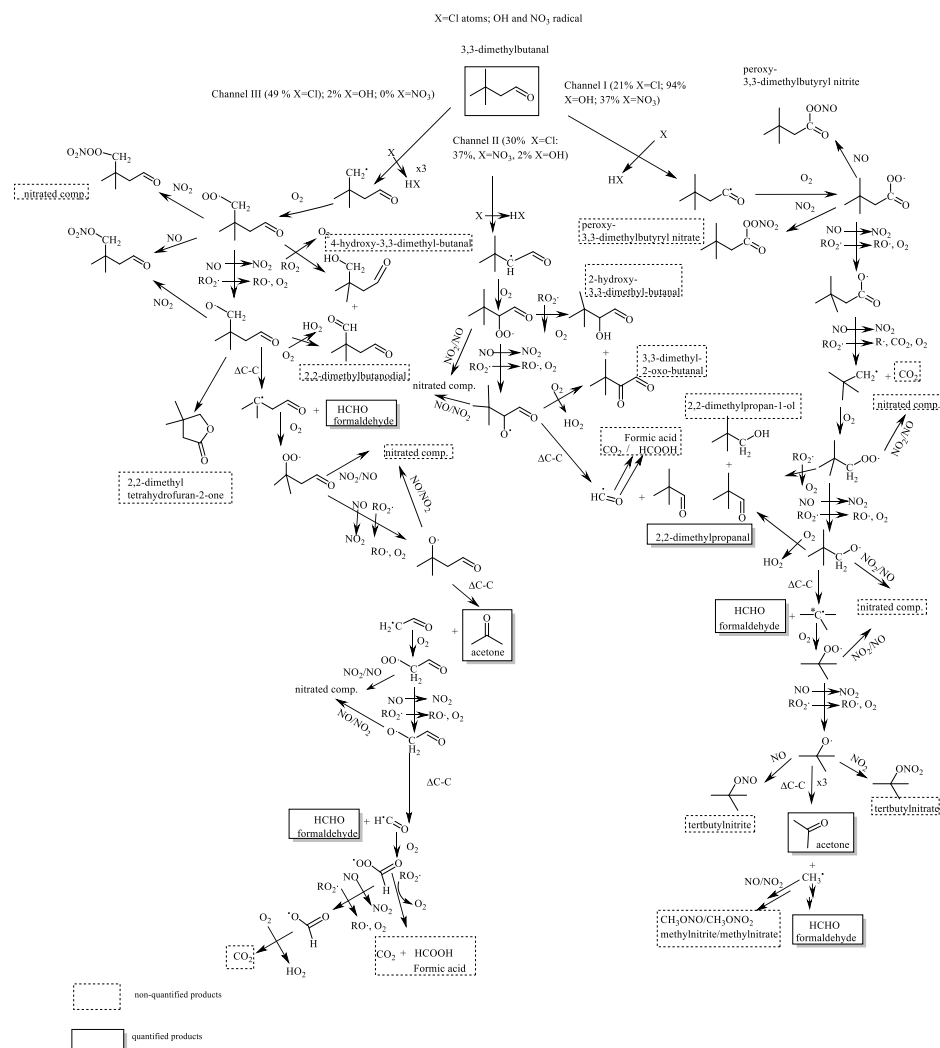
589 The total carbon calculated for the Cl reaction in the absence of NO, based on the yields of HCHO, acetone, and
590 22DMpropanal, accounts for only 45%. The remaining carbon can be explained by the formation of other
591 compounds identified through SPME/GC-TOFMS. Additionally, the IR band at 1105 cm⁻¹ shown in Figure 11S in
592 the FTIR spectrum of the Cl atoms reaction in the absence of NO, indicates the formation of formic acid, which was
593 not quantified. The lower yields in the Cl reaction in the presence of NO (33%) and OH (16%) could be attributed
594 to the significant formation of nitrated compounds, whose yield has not been included in the total carbon calculation.
595 For the NO₃ radical reaction, the linear trend observed in Figure 5 indicates that nitrated compounds are formed
596 through the main reaction, and therefore, 100% of the reacted 33DMbutanal forms nitrated compounds in this
597 reaction conditions. The identification of other compounds in the SPME/GC-TOFMS analysis could be due to the
598 rapid decomposition of peroxy nitrated compounds in the chromatograph's injection port or an overestimation of
599 nitrated compound yields. To determine if these products are generated in significant amounts, quantification is
600 necessary, but this is not possible due to the lack of standards or the characteristics of the SPME sampling method.

601 No exclusive compounds to each reaction channel (I, II, or III) have been quantified for 33DMbutanal reaction.
602 Therefore, it is not possible to determine the percentage of each channel through which the reaction of 3,3DMbutanal
603 with each oxidant proceeds. The formation of 33DMbutanoic acid in all reactions implies other reaction pathway
604 that has not been considered. The following reaction has been proposed as possible pathways to explain the
605 formation of the 3,3-dimethylbutanoic acid ((CH₃)₃CCH₂C(O)OH):



607 Similar reaction was proposed for $\text{CH}_3\text{C}(\text{O})\text{OO}$ radical by some authors (Dillon and Crowley 2008, Groß et al.,
608 2014, Tomas et al., 2001). On the other hand, 22DMpropanoic acid (observed in the 33DMbutanal with Cl atoms)
609 could be a secondary product formed from the degradation of 22DMpropanal. The yields of organic acids from the
610 corresponding aldehyde must be very low (Bo et al. 2022), and therefore, the pathway (R2) must be a minority
611 channel.

612 From the analysis of the SPME/GC-TOFMS experiments, the proposed reaction products are also listed in Table 3.
613 Based on the products identified in this work, the previous bibliographic study of 33DMbutanal with the OH radical
614 (Aschmann et al. 2010) and considering the estimated percentages for each channel using the SAR method, the
615 reaction mechanism for 33DMbutanal with Cl atoms, OH and NO_3 radicals showed in Figure 9, is proposed to
616 explain the main observed reaction products in each reaction.



617

618 Figure 8: Mechanism proposed by the formation of the main reaction products observed for 33DMbutanal reaction
 619 with Cl atoms, OH and NO₃ radical. The framed products correspond to products identified by FTIR and/or
 620 SPME/GC-TOFMS.

621 **4 Atmospheric Implications**

622 The atmospheric implications of the degradation of 33DMbutanone and 33DMbutanal are determined based on their
 623 lifetimes, the effects of the reaction products generated, their influence on global warming and air quality, and
 624 consequently, their impact on health and living organisms.

625 The lifetime of a species in the atmosphere is calculated based on its degradation rate through various chemical
 626 processes, such as reactions with oxidants, photolysis, or deposition. In general, to estimate the atmospheric lifetime
 627 with respect to homogeneous chemical reactions with oxidants, the Eq. (II) is used:



$$\tau_{ox} = \frac{1}{k_{ox}[Ox]} \quad (II)$$

where τ_{ox} represents the lifetime for the considered reaction, k_{ox} is the rate coefficient, and $[Ox]$ refers to the typical atmospheric concentration of the oxidant. The atmospheric lifetimes of 33DMbutanone and 33DMbutanal were calculated using the rate coefficients of Table 2. For 33DMbutanal the k_{OH} and k_{NO_3} have been averaged from the two rate coefficients available in the literature.

The ketones and aldehydes can significantly absorb light in the tropospheric actinic region $\lambda > 290$ nm, and the photolysis could play an important degradation process (Atkinson, 2003; Mellouki et al., 2015). There are not any experimental data about UV-Vis absorption cross-sections of 33DMbutanal that could allow the calculation of the photolysis rate. The value of $J(0, \theta) = 3 \times 10^{-5} \text{ s}^{-1}$ calculated for 3-methyl-butanal (similar compound to 33DMbutanal) by Lanza et al., (2008), has been used to estimate the photolysis lifetime. For 33DMbutanone a photolysis rate of $J(z, \theta) = 2.4 \times 10^{-6} \text{ s}^{-1}$. was estimated by Mapelli et al. (2023).

Respecting to deposition process the lifetime associated with wet deposition could be estimated with the Eq. (III) proposed by (Chen et al., 2003):

$$\tau_{wet} = \frac{H_{atm}}{k_H v_{pm} RT} \quad (III)$$

where k_H is the Henry's law constant; H_{atm} is the height in the troposphere ($H_{atm} = 630$ m), v_{pm} is the average precipitation rate (536 mm yr^{-1} for Spain, (<http://www.aemet.es>, last access: 4 October 2024), R is the gas constant ($8.14 \text{ Pa m}^3/\text{mol K}$); and T is the temperature, considered to be constant and equal to 298 K. In the literature, there is only one data of Henry's constant for 33DMButanone of $4.3 \times 10^{-2} \text{ mol/m}^3\text{Pa}$ (Hovorka et al., 2019, Sander, 2023). The same data has been used to 33DMbutanal.

Taking into account all those degradation processes, a global lifetime (τ_{global}) has also been calculated for 33DMbutanone and 33DMbutanal with the equation (IV):

$$\tau_{global} = \left[\frac{1}{\tau_{Cl}} + \frac{1}{\tau_{OH}} + \frac{1}{\tau_{NO_3}} + \frac{1}{\tau_{phot}} + \frac{1}{\tau_{wet}} \right]^{-1} \quad (IV)$$

Table 5. Atmospheric lifetimes of 33DMButanone and 33DMButanal.

	^a τ_{Cl} (days)	τ_{Cl}^* (days)	^b τ_{OH} (days)	^c τ_{NO_3} (days)	τ_{phot} (days)	τ_{wet} (years)	τ_{global} (days)	^e τ_{global} (days)
33DMbutanal	91	0.7	0.5	1.2	0.4 ^d	11	0.2	0.14
33DMbutanone	274	2.1	9.2	-	5 ^e	11	2.5	1.14

^aDetermined using the 24 h average $[Cl] = 1 \times 10^3 \text{ atoms cm}^{-3}$ (global average) (Platt and Jansen, 1995). ^{*}Determined using the peak of $[Cl]$ in coastal and industrial areas at $1.3 \times 10^5 \text{ atoms cm}^{-3}$ (Spicer et al., 1998). ^b Determined using the 12 h average of $[OH] = 1 \times 10^6 \text{ radicals cm}^{-3}$ (12-hour average) (Prinn et al., 2001), $[NO_3] = 5 \times 10^8 \text{ radicals cm}^{-3}$ (Atkinson, 2000). ^dData calculated with a J from Lanza et al., 2008. ^eData calculated with a J from Mapelli et al., 2023.

It can be observed that the dominant tropospheric loss processes of 33DMbutanone and 33DMbutanal are their reactions with OH radicals and photolysis process (Note that photolysis lifetime depends on the atmospheric conditions considered), followed by their reaction with NO_3 radicals at night. However, in places where there is a



658 peak concentration of Cl atoms (coastal areas), the reaction with Cl atoms may compete with photolysis and reaction
659 with OH radicals as their main degradation process. The calculated wet lifetime of 11 years indicate that the wet
660 deposition can be considered negligible.

661 The shorter global lifetime of ~4 hours for 33DMbutanal and ~ 2 days for 33DMbutanone indicate that these
662 compounds are degraded near their generation sources. The products created in the degradation reactions of
663 33DMbutanone and 33DMbutanal may also have environmental implications. Thus, formaldehyde is classified as
664 potentially carcinogenic to humans (NTP, 2021). Acetone, 22DMpropanal and organic nitrates (PAN and
665 peroxybutyrylnitrate) are also key components in photochemical smog episodes, a major contemporary
666 environmental issue. The multifunctional compounds such as oxocarbonyls, dicarbonyls, hydroxycarbonyls and
667 acids are products with polar groups characterized by low volatility, which could facilitate the formation of
668 secondary organic aerosols (SOA) (Calvert et al., 2011, Asensio et al. 2022). Moreover, the nitrated compounds
669 generated can act as NO_x reservoir species, especially during the night (Altshuller, 1993) and could have an
670 influence at the global scale.

671 The potential for ozone formation of 33DMbutanone and 33DMbutanal has been evaluated calculating their
672 Photochemical Ozone Creation Potential (POCP) according with the method of Jenkin et al., (2017). The
673 Photochemical Ozone Creation Potential estimated (POCP_E), were 68 and 58 for conditions in NW Europe and
674 urban areas of the USA, respectively for 33DMbutanal and 26 and 15 for conditions in NW Europe and urban areas
675 of the USA, respectively for 33DMbutanone. Comparing with other series of organic compounds (Jenkin et al.,
676 2017), the values of POCP_E for 33DMbutanal indicate that it is an important contributor to tropospheric ozone
677 generation.

678 Regarding the calculation of the GWP (global warming potential) parameter, the method of Hodnebrog et al., (2020)
679 and the lifetime calculated above have been used to estimate the GWP of 33DMbutanone. A value of 0.13 for a time
680 horizon of 20 years has been obtained, and therefore, the direct contribution to the radiative forcing of climate can
681 be considered negligible. The GWP for 33DMbutanal has not been calculated because its lifetime is shorter than
682 that of 33DMbutanone, and thus, its expected GWP is likely to be lower.

683 **5 Conclusions**

684 In this work, the rate coefficient for the reaction of 33DMbutanal with Cl atoms has been determined for the first
685 time. Additionally, the rate coefficients for 33DMbutanone with Cl atoms and the OH radical have been measured,
686 aligning with existing literature data. The kinetic findings, along with previous studies on other carbonyl compounds,
687 confirm that reactivity is influenced by the type of carbonyl group (aldehyde vs. ketone) and the number and position
688 of methyl groups. This research has expanded the database on these compounds, especially regarding their reactions
689 with Cl atoms.

690 The study of reaction products using FTIR and GC-MSTOF allows to identify and quantify acetone, formaldehyde,
691 and 22DMpropanal, alongside multifunctional products like hydroxycarbonyls, oxocarbonyls, and nitrated
692 compounds such as PAN and peroxybutyryl nitrate. The results suggest that the RO₂ + OH· reaction in the unpolluted
693 atmosphere could be significant. The proposed mechanism for 33DMbutanone indicates that hydrogen abstraction
694 from the tert-butyl methyl group is the primary pathway for Cl and OH, confirming SAR predictions. In the
695 33DMbutanal reaction, hydrogen abstraction occurs from various functional groups depending on the reacting



696 species (Cl atoms, NO₃, and OH radicals), also aligning with SAR predictions. The positive identification of
697 33DMbutanoic acid implies a pathway in the reaction mechanisms of 33DMbutanal, that initially have not been
698 considered.

699 The atmospheric conditions determine the reaction products obtained in the atmospheric degradation of
700 33DMbutanal and 33DMbutanone. Thus, in polluted environments with high concentrations of NO_x, nitrated
701 organic compounds (RONO₂) are formed. Moreover, when the concentration of NO₂ is higher than that of NO,
702 ozone is formed. In a clean atmosphere, as in the case of the experiments with Cl atoms in the absence of NO_x, the
703 reaction products are hydroxy/oxo carbonyl compounds.

704 Atmospherically, both 33DMbutanal and 33DMbutanone degrade within a few hours and 2 days respectively during
705 the day, implying that degradation happens close to the emission sources. Their direct contribution to radiative
706 forcing is minimal. However, their estimated POCP values suggest a potential role in tropospheric ozone formation,
707 especially for 33DMbutanal. The multifunctional products formed may contribute to secondary organic aerosol
708 formation, and their further oxidation in the troposphere could enhance photochemical smog, impacting air quality
709 and human health.

710 **Data availability.** The underlying research data are available upon email request from the contact author of this
711 work.

712 **Supplement.** The electronic Supplement includes additional tables and figures.

713 **Author contributions.**

714 **Inmaculada Aranda:** Formal analysis, validation, investigation, methodology, writing-original draft. **Pilar**
715 **Martín:** Conceptualization, supervision, methodology, writing-original draft; **Sagrario Salgado** Conceptualization,
716 supervision, methodology, writing-original draft. **Florentina Villanueva:** Supervision, methodology. **Beatriz**
717 **Cabañas:** Conceptualization, supervision, funding acquisition.

718 **Competing interests**

719 The contact author has declared that none of the authors has any competing interests.

720 **Acknowledgments**

721 The authors thank for financial support. I. Aranda thanks UCLM for funding her research contract (Plan Propio de
722 I+D+i) cofinanced by FSE.

723 **Financial support.** This research has been supported by the Ministry of Science, Innovation and Universities
724 (Project RTI 2018-099503-B-I00) and the Junta de Comunidades de Castilla-La Mancha (Project SBPLY/21/180501
725 /000283).

726 **References**

727 -Altshuller, A. P.: PANs in the Atmosphere, Air & Waste, 43, 1221–1230,
728 <https://doi.org/10.1080/1073161X.1993.10467199>, 1993.



- 729 -Aranda, I., Salgado, S., Martín, P., Villanueva, F., Pinés, M.T., Cabañas, B.: Atmospheric degradation of 2-
730 Isopropoxyethanol: Reactions with Cl, OH and NO₃, Atmos. Environ., 324-329,
731 <https://doi.org/10.1016/j.atmosenv.2024.120420>, 2024.
- 732 -Aranda, I., Salgado, S., Martín, P., Villanueva, F., Martinez, E., Cabañas, B: Atmospheric degradation of 3-ethoxy-
733 1-propanol by reactions with Cl, OH and NO₃, Chemosphere, 281, 130755-130764,
734 <https://doi.org/10.1016/j.chemosphere.2021.130755>, 2021.
- 735 -Aschmann, S. M., Arey J., Atkinson, R: Kinetics and Products of the Reactions of OH Radicals with 4,4-Dimethyl-
736 1-pentene and 3,3-Dimethylbutanal at 296 ± 2 K, J. Phys. Chem. A, 114, 18, 5810–5816,
737 <https://doi.org/10.1021/jp101893g>, 2010.
- 738 -Asensio, M., Antiñolo, M., Blázquez, S., Albaladejo, J., and Jiménez, E.: Evaluation of the daytime tropospheric
739 loss of 2-methylbutanal, Atmos. Chem. Phys., 22, 2689–2701, <https://doi.org/10.5194/acp-22-2689-2022>, 2022.
- 740 -Atkinson, R., Rate constants for the atmospheric reactions of alkoxy radicals: An updated estimation method,
741 Atmos. Environ., 41, Issue 38, 8468-8485, <https://doi.org/10.1016/j.atmosenv.2007.07.002>, 2007.
- 742 -Atkinson, R.: Atmospheric Degradation of Volatile Organic Compounds. Chem. Rev.103, 12, 4605–4638,
743 <https://doi.org/10.1021/cr0206420>, 2003.
- 744 -Atkinson, R.: Atmospheric chemistry of VOCs and NO(x). Atmos. Environ. 34, 2063–2101.
745 [https://doi.org/10.1016/S1352-2310\(99\)00460-4](https://doi.org/10.1016/S1352-2310(99)00460-4), 2000.
- 746 -Atkinson, R., Arey J., Aschmann S. M: Atmospheric chemistry of alkanes: Review and recent developments.
747 Atmos. Environ. 42(23),5859–5871, <https://doi.org/10.1016/j.atmosenv.2007.08.040>, 2008.
- 748 -Bao, J., Li, H., Wu, Z., Zhang, X., Zhang, H., Li, Y., Qian, J., Chen, J., Deng, L: Atmospheric carbonyls in a heavy
749 ozone pollution episode at a metropolis in Southwest China: Characteristics, health risk assessment, sources analysis,
750 J. Environ. Sci (China), 113, 40-54, <https://doi.org/10.1016/j.jes.2021.05.029>, 2022.
- 751 -Berndt, T., Scholz, W., Mentler, B., Fischer, L., Herrmann, H., Kulmala, M., Hansel, A., Accretion Product
752 Formation from Self- and Cross-Reactions of RO₂ Radicals in the Atmosphere. Angew. Chem. Int. Ed.
753 26;57(14):3820-3824. <https://doi.org/10.1002/anie.201710989>, 2018.
- 754 -Bo, S., Weigang, W., Cici, F., Yuchan, Z., Zheng, S., Yanli, Z., Maofa, G.: Study on the reaction of 3-methyl-2-
755 butenal and 3-methylbutanal with Cl atoms: kinetics and reaction mechanism, J. Environ. Sci., 116, 2022, 25-33,
756 <https://doi.org/10.1016/j.jes.2021.03.032>, 2022.
- 757 -Bottorff, B., Lew, M. M., Woo, Y., Rickly, P., Rollings, M. D., Deming, B., Anderson, D. C., Wood, E., Alwe, H.
758 D., Millet, D. B., Weinheimer, A., Tyndall, G., Ortega, J., Dusanter, S., Leonardis, T., Flynn, J., Erickson, M.,
759 Alvarez, S., Rivera-Rios, J. C., Shutter, J. D., Keutsch, F., Helmig, D., Wang, W., Allen, H. M., Slade, J. H., Shepson,
760 P. B., Bertman, S., and Stevens, P. S.: OH, HO₂, and RO₂ radical chemistry in a rural forest environment:
761 measurements, model comparisons, and evidence of a missing radical sink, Atmos. Chem. Phys., 23, 10287–10311,
762 <https://doi.org/10.5194/acp-23-10287-2023>, 2023.



- 763 -Byrne, F. P., Forier, B., Bossaert, G., Hoebers, C., Farmer, T. J., and Hunt, A. J.: A methodical selection process
764 for the development of ketones and esters as bio-based replacements for traditional hydrocarbon solvents, *Green*
765 *Chem.*, 20, 4003–4011, <https://doi.org/10.1039/C8GC01132J>, 2018.
- 766 -Calvert, J.G., Mellouki, A., Orlando, J.J., Pilling, M.J., Wallington, T.J.: *The Mechanisms of Atmospheric*
767 *Oxidation of the Oxygenates*. Oxford University Press, New York, 2011.
- 768 -Carter, W.P.L. Estimation of Rate Constants for Reactions of Organic Compounds under Atmospheric Conditions.
769 *Atmosphere*, 12, 1250. <https://doi.org/10.3390/atmos12101250>, 2021.
- 770 -Chen, L., Takenaka, N., Bandow, H., Maeda, Y.: Henry's law constants for C2–C3 fluorinated alcohols and their
771 wet deposition in the atmosphere, *Atmos. Environ.*, 37, 34, 4817-4822,
772 <https://doi.org/10.1016/j.atmosenv.2003.08.002>, 2003.
- 773 -Colmenar, I., Martín, P., Cabanas, B., Salgado, S., Tapia, A., Aranda, I., Atmospheric fate of a series of saturated
774 alcohols: kinetic and mechanistic study. *Atmos. Chem. Phys.* 20, 699–720. [https://doi.org/10.5194/acp-20-699-](https://doi.org/10.5194/acp-20-699-2020)
775 [2020](https://doi.org/10.5194/acp-20-699-2020), 2020a.
- 776 -Colmenar, I., Salgado, S., Martín, P., Aranda, I., Tapia, A., Cabanas, B., 2020b. Tropospheric reactivity of 2-
777 ethoxyethanol with OH and NO₃ radicals and Cl atoms. Kinetic and mechanistic study. *Atmos. Environ.* 224,
778 117367. <https://doi.org/10.1016/j.atmosenv.2020.117367>., 2020b.
- 779 -Colmenar, I., Martín, P., Cabanas, B., Salgado, S., Martínez, E.: Analysis of reaction products formed in the gas
780 phase reaction of E,E-2,4-hexadienal with atmospheric oxidants: reaction mechanisms and atmospheric
781 implications. *Atmos. Environ.* 176, 188–200. <https://doi.org/10.1016/j.atmosenv.2017.12.027>, 2018.
- 782 -D'Anna, B., Andresen, W., Gefen, Z., and Nielsen, C. J.: Kinetic study of OH and NO₃ radical reactions with 14
783 aliphatic aldehydes, *Phys. Chem. Chem. Phys.*, 3, 3057–3063, doi.org/10.1039/B103623H, 2001.
- 784 -D'Anna and Nielsen 1997. Kinetic study of the vapour-phase reaction between aliphatic aldehydes and the nitrate
785 radical. *J. Chem. Soc., Faraday Trans.*, 93(19), 3479–3483, <https://doi.org/10.1039/A702719B>, 1997.
- 786 -Dillon, T. J. and Crowley, J. N.: Direct detection of OH formation in the reactions of HO₂ with CH₃C(O)O₂ and
787 other substituted peroxy radicals, *Atmos. Chem. Phys.*, 8, 4877–4889, <https://doi.org/10.5194/acp-8-4877-2008>,
788 2008.
- 789 -EUROCHAMP, 2020 <https://data.eurochamp.org/data-access/ir-spectra/#/>
- 790 -Farrugia, L. N., Bejan, I., Smith, S. C., Medeiros, D. J., and Seakins, P. W.: Revised structure activity parameters
791 derived from new rate coefficient determinations for the reactions of chlorine atoms with a series of seven ketones
792 at 290 K and 1 atm, *Chem. Phys. Lett.*, 640 87–93, <https://doi.org/10.1016/j.cplett.2015.09.055>, 2015.
- 793 -Finlayson-Pitts, B. J., Pitts, Jr. J. N.: *Chemistry of the Upper and Lower Atmosphere: Theory, Experiments, and*
794 *Applications*. Academic Press, 2000.



- 795 -Fittschen, C. The reaction of peroxy radicals with OH radicals, *Chem. Phys. Lett.*, 725, 102-108,
796 <https://doi.org/10.1016/j.cplett.2019.04.002>, 2019.
- 797 - Groß, C. B. M., Dillon, T. J., Schuster, G., Lelieveld, J., and Crowley, J. N.: Direct kinetic study of OH and O₃
798 formation in the reaction of CH₃C(O)O₂ with HO₂, *The Journal of Physical Chemistry A*, 118, 974-985,
799 <https://doi.org/10.1021/jp412380z>, 2014.
- 800 -Glasius, M., Calogirou, A., Jensen, N., Hjorth, J., Nielsen, C.: Kinetic Study of Gas Phase Reactions of
801 Pinonaldehyde and Structurally Related Compounds. *Int. J. Chem. Kinet.* 7; 527-533,
802 [https://doi.org/10.1002/\(SICI\)1097-4601\(1997\)29:7<527::AID-KIN7>3.0.CO;2-W](https://doi.org/10.1002/(SICI)1097-4601(1997)29:7<527::AID-KIN7>3.0.CO;2-W), 1997.
- 803 -Heald, C. L.; Kroll, J. H. The Fuel of Atmospheric Chemistry: Toward a Complete Description of Reactive Organic
804 Carbon. *Sci. Adv.*, 6, 8967, <https://doi.org/10.1126/sciadv.aay8967>, 2020.
- 805 -Hodnebrog, Ø., Aamaas, B., Fuglestedt, J. S., Marston, G., Myhre, G., Nielsen, C. J., et al. Updated global warming
806 potentials and radiative efficiencies of halocarbons and other weak atmospheric absorbers. *Reviews of Geophysics*,
807 58, e2019RG000691, <https://doi.org/10.1029/2019RG000691>, 2020.
- 808 -Hovorka, Š., Vrbka, P., Bermúdez-Salguero, C., Böhme, A., & Dohnal, V.: Air–water partitioning of C₅ and C₆
809 alkanones: measurement, critical compilation, correlation, and recommended data, *J. Chem. Eng. Data*, 64, 5765–
810 5774, <https://doi.org/10.1021/ACS.JCED.9B00726>, 2019.
- 811 -IUPAC. Task Group on Atmospheric Chemical Kinetic. <http://iupac.pole-ether.fr>, 2007.
- 812 -Jenkin, M.E., Derwent, R.G., Wallington, T.J.: Photochemical ozone creation potentials for volatile organic
813 compounds: Rationalization and estimation. *Atmos. Environ.* 163, 128–137.
814 <https://doi.org/10.1016/j.atmosenv.2017.05.024>, 2017.
- 815 -Jenkin, M. E., Saunders, S. M., and Pilling, M. J.: The tropospheric degradation of volatile organic compounds: a
816 protocol for mechanism development, *Atmos. Environ.*, 31, 81–104, [https://doi.org/10.1016/S1352-2310\(96\)00105-](https://doi.org/10.1016/S1352-2310(96)00105-7)
817 [7](https://doi.org/10.1016/S1352-2310(96)00105-7), 1997.
- 818 -Kerdouci, J., Picquet-Varrault, B., Doussin, J.F: Structure–activity relationship for the gas-phase reactions of NO₃
819 radical with organic compounds: Update and extension to aldehydes. *Atmos. Environ.* 2014, 84, 363–372,
820 <https://doi.org/10.1016/j.atmosenv.2013.11.024>, 2014.
- 821 -Kwok, E.S.C., Atkinson, R. Estimation of hydroxyl radical reaction rate constants for gas-phase organic compounds
822 using a structure-reactivity relationship: An update. *Atmos. Environ.* 29, 1685-1695, [https://doi.org/10.1016/1352-](https://doi.org/10.1016/1352-2310(95)00069-B)
823 [2310\(95\)00069-B](https://doi.org/10.1016/1352-2310(95)00069-B), 1995.
- 824 -Lanza, B., Jiménez, E., Ballesteros, B., Albaladejo, J: Absorption cross section determination of biogenic C₅-
825 aldehydes in the actinic region, *Chem. Phys. Lett.*, 454, 184-189, <https://doi.org/10.1016/j.cplett.2008.02.020>, 2008.
- 826 -Liu, Q., Gao, Y., Huang, W., Ling, Z., Wang, Z., Wang, X.: Carbonyl compounds in the atmosphere: A review of
827 abundance, source and their contributions to O₃ and SOA formation, *Atmos. Res.*, 274, 106184,
828 <https://doi.org/10.1016/j.atmosres.2022.106184>, 2022.



- 829 -Mapelli, C., Donnelly, J. K., Hogan, Ú. E., Rickard, A. R., Robinson, A. T., Byrne, F., McElroy, C. R., Curchod,
830 B. F. E., Hollas, D., and Dillon, T. J.: Atmospheric oxidation of new 'green' solvents part II: methyl pivalate and
831 pinacolone. *Atmos. Chem. Phys.*, 23, 7767–7779, <https://doi.org/10.5194/acp-23-7767-2023>, 2023.
- 832 -McGillen, M. R., Carter, W. P. L., Mellouki, A., Orlando, J. J., Picquet-Varrault, B. and Wallington T. J. "Database
833 for the kinetics of the gas-phase atmospheric reactions of organic compounds," *Earth Syst. Sci. Data*, 12, 1203–
834 1216, <https://doi.org/10.5194/essd-12-1203-2020>, 2020.
- 835 -Mellouki, A., Wallington, T. J., and Chen, J.: Atmospheric chemistry of oxygenated volatile organic compounds:
836 impacts on air quality and climate, *Chem. Rev.*, 115, 3984–4014, <https://doi.org/10.1021/cr500549n>, 2015.
- 837 -NTP (National Toxicology Program). Report on Carcinogens, Fifteenth Edition. Research Triangle Park, NC: U.S.
838 Department of Health and Human Services, Public Health Service, doi.org/10.22427/NTP-OTHER-1003_2021.
- 839 -Platt, U., Jansen, C.: Observation and role of the free radicals NO₃, ClO, BrO and IO in the troposphere. *Faraday*
840 *Discuss* 100, 175–198. <https://doi.org/10.1039/FD9950000175>, 1995.
- 841 -Prinn, R.G., Huang, J., Weiss, R.F., Cunnold, D.M., Fraser, P.J., Simmonds, P.G., McCulloch, A., Harth, C.,
842 Salameh, P., O'Doherty, S., Wang, R.H.J., Porter, L., Miller, B.R.: Evidence for Substantial Variations of
843 Atmospheric Hydroxyl Radicals in the Past Two Decades. *Science*. 292, 1882–1888.
844 doi.org/10.1126/science.1058673, 2001.
- 845 -Ren, Y., Wang, J., Grosselin, B., Daele, V., and Mellouki, A.: Kinetic and product studies of Cl atoms reactions
846 with a series of branched ketones, *J. Environ. Sci.*, 71, 271–282, <https://doi.org/10.1016/j.jes.2018.03.036>, 2018.
- 847 -Ródenas, M. IR spectrum: FORMALDEHYDE HCHO (Version 1.0) [Data set]. AERIS. [https://doi.org](https://doi.org/10.25326/K17C-0762)
848 [/10.25326/K17C-0762](https://doi.org/10.25326/K17C-0762), 2017.
- 849 -Sander, R.: Compilation of Henry's law constants (version 5.0.0) for water as solvent, *Atmos. Chem. Phys.*, 23,
850 10901–12440, <https://doi.org/10.5194/acp-23-10901-2023>, 2023.
- 851 -Saunders, S. M., Jenkin, M. E., Derwent, R. G., and Pilling, M. J.: Protocol for the development of the Master
852 Chemical Mechanism, MCM v3 (Part A): tropospheric degradation of non-aromatic volatile organic compounds,
853 *Atmos. Chem. Phys.*, 3, 161–180, <https://doi.org/10.5194/acp-3-161-2003>, 2003
- 854 -Schott, G., Davidson, N.: Shock Waves in Chemical Kinetics: The Decomposition of N₂O₅ at High Temperatures.
855 *J. Am. Chem. Soc.* 80, 1841–1853. <https://doi.org/10.1021/ja01541a019>, 1958.
- 856 -Singh, S., Hernandez, S., Ibarra, Y., Hasson, A.S.: Kinetics and mechanism of the reactions of n-butanal and n-
857 pentanal with chlorine atoms. *Int. J. Chem. Kinet* 41: 133-141, <https://doi.org/10.1002/kin.20383>, 2009.
- 858 -Spicer, C.W., Chapman, E.G., Finlayson-Pitts, B.J., Plastringe, R.A., Hubbe, J.M., Fast, J.D., Berkowitz,
859 C.M.: Unexpected high concentrations of molecular chlorine in coastal air. *Nature* 394, 353–356.
860 <https://doi.org/10.1038/28584>, 1998.



- 861 -Tadic, J. M., Moortgat, G. K., Bera, P. P., Loewenstein, M., Yates, E. L., and Lee, T. J.: Photochemistry and
862 photophysics of n-butanal, 3-methylbutanal, and 3,3 dimethylbutanal: Experimental and theoretical study, *J. Phys.*
863 *Chem. A*, 116, 5830–5839, <https://doi.org/10.1021/jp208665v>, 2012.
- 864 -Tanielyan, S.K. and Augustine, R.L.: Synthesis of 3,3-dimethylbutanol and 3,3-dimethylbutanal, important
865 intermediates in the synthesis of Neotame. *Top Catal.*, 55, 625-630, <https://doi.org/10.1007/s11244-012-9841-z>,
866 2012.
- 867 -Taylor, W.D., Allston, T.D., Moscato, M.J., Fazekas, G.B., Kozlowski, R., Takacs, G.A.: Atmospheric
868 photodissociation lifetimes for Nitromethane, Methyl Nitrite and Methyl Nitrate. *Int. J. Chem. Kinet.* 12, 4, 231–
869 240. <https://doi.org/10.1002/kin.550120404>, 1980.
- 870 -Tomas, A., Villenave, E., and Lesclaux, R.: Reactions of the HO₂ radical with CH₃CHO and CH₃C(O)O₂ in the
871 gas phase, *J. Phys. Chem. A*, 105, 3505–3514, <https://doi.org/10.1021/jp003762p>, 2001.
- 872 -Tuazon, E.C., Atkinson, R.: A product study of the gas-phase reaction of Isoprene with the OH radical in the
873 presence of NO_x. *Int. J. Chem. Kinet.* 22, 1221–1236, <https://doi.org/10.1002/kin.550221202>, 1990.
- 874 -Tuazon, E. C., Leod, H. M., Atkinson, R., and Carter, W. P. L.: α -Dicarbonyl Yields from the NO_x Air
875 Photooxidations of a Series of Aromatic Hydrocarbons in Air, *Environ. Sci. Technol.*, 20, 383–387,
876 <https://doi.org/10.1021/es00146a010>, 1986.
- 877 -US EPA. [2024]. Estimation Programs Interface Suite™ for Microsoft® Windows, v 4.11 or insert version used].
878 United States Environmental Protection Agency, Washington, DC, USA.
- 879 -Vereecken L and Peeters J. A structure–activity relationship for the rate coefficient of H-migration in substituted
880 alkoxy radicals. *Phys. Chem. Chem. Phys.*, 12, 12608–12620, <https://doi.org/10.1039/C0CP00387E>, 2010.
- 881 -Vereecken L and Peeters J. Decomposition of substituted alkoxy radicals—part I: a generalized structure–activity
882 relationship for reaction barrier heights. *Phys. Chem. Chem. Phys.*, 11, 9062–9074,
883 <https://doi.org/10.1039/B909712K>, 2009.
- 884 -Vila, J.A., Argüello, G.A., Malanca, F.E. Kinetics studies of 5-methyl-2-hexanol, 2,2-dimethyl-3-hexanol, and
885 2,4,4-trimethyl-1-pentanol with chlorine atoms: Photooxidation mechanism of 2,4,4-trimethyl-1-pentanol. *Int. J.*
886 *Chem. Kinet.*, 52(1), 29-34, <https://doi.org/10.1002/kin.21327>, 2020.
- 887 -Wallington, T. J. and Kurylo, M. J.: Flash Photolysis Resonance Fluorescence Investigation of the Gas-Phase
888 Reactions of OH Radicals with a Series of Aliphatic Ketones over the Temperature Range 240–440 K, *J. Phys.*
889 *Chem.*, 91, 5050–5054, <https://doi.org/10.1021/j100303a033>, 1987.
- 890 -Xiong, K., Zheng, X., Jiang, M., Gao, D., Wang, F., and Chen y. Phase Equilibrium on Extraction Methylphenols
891 from Aqueous Solution with 3,3-Dimethyl-2-butanone at 333.2 K and 353.2 K. *J. Chem. Eng. Data*, 63, 7, 2376–
892 2383, <https://doi.org/10.1021/acs.jced.7b00932>, 2018.



- 893 -Zhou, X., Zhou, X., Wang, C., Zhou, H. Environmental and human health impacts of volatile organic compounds:
894 A perspective review, Chemosphere, 313, <https://doi.org/10.1016/j.chemosphere.2022.137489>, 2023.